

N 7 3 25 8 8 6

NASA TECHNICAL  
MEMORANDUM

NASA TM X-64665

CASE FILE  
COPY

RESEARCH ROCKET TESTS RR-1 (BLACK BRANT VC)  
AND RR-2 (AEROBEE 170A): INVESTIGATIONS OF  
THE STABILITY OF BUBBLES IN PLAIN AND  
FIBER-REINFORCED METAL MELTED AND SOLIDIFIED  
IN A NEAR-ZERO-g ENVIRONMENT

By I. C. Yates and Vaughn H. Yost  
Process Engineering Laboratory

June 1973 (Revised Edition)

NASA

*George C. Marshall Space Flight Center  
Marshall Space Flight Center, Alabama*

1. REPORT NO. TM X-64665		2. GOVERNMENT ACCESSION NO.		3. RECIPIENT'S CATALOG NO.	
4. TITLE AND SUBTITLE Research Rocket Tests RR-1 (Blank Brant VC) and RR-2 (Aerobee 170A): Investigations of the Stability of Bubbles in Plain and Fiber-Reinforced Metal Melted and Solidified in a Near-Zero-g Environment				5. REPORT DATE June 1973 (Revised Edition)	
				6. PERFORMING ORGANIZATION CODE	
7. AUTHOR(S) I. C. Yates and Vaughn H. Yost				8. PERFORMING ORGANIZATION REPORT #	
9. PERFORMING ORGANIZATION NAME AND ADDRESS George C. Marshall Space Flight Center Marshall Space Flight Center, Alabama 35812				10. WORK UNIT NO.	
				11. CONTRACT OR GRANT NO.	
12. SPONSORING AGENCY NAME AND ADDRESS National Aeronautics and Space Administration Washington, D.C. 20546				13. TYPE OF REPORT & PERIOD COVERED Technical Memorandum	
				14. SPONSORING AGENCY CODE	
15. SUPPLEMENTARY NOTES Prepared by Process Engineering Laboratory, Science and Engineering					
16. ABSTRACT <p>This report contains the results of the first two of a series of research rocket flights. The objectives of these flights were (1) to learn about the capabilities of these rockets, (2) to learn how to interface the payloads and rockets, and (3) to process some of the composite casting demonstration capsules intended originally for Apollo 15. The capsules contained experiments for investigating the stability of gas bubbles in plain and fiber-reinforced metal melted and solidified in a near-zero-g (0.0119g) environment. The characteristics of the two research rockets, an Aerobee 170A and a Black Brant VC, used to obtain the periods of near-zero-g and the Temperature Control Unit used for processing the contents of the two experiment capsules are discussed in detail. Flight data for the Aerobee 170A NASA 13. 113 are presented and analyzed.</p> <p>The first two objectives were met and the third partially fulfilled. The acceleration produced by coning (precession) after yo-yo despin of the Aerobee rocket was insignificant (<math>8 \times 10^{-7}g</math>) compared to that produced by the final spin rate (<math>1.8 \times 10^{-3}g</math>). The capsule contents tended to pull away from the capsule walls as they melted, causing incomplete melting and decreasing the effectiveness of the water quench cooling system. In areas where melting occurred the bubbles appeared to be much more stable than those in an identical capsule processed in one-g.</p> <p>For future experiments, the capsule interiors should be plated with some material that does not repel the capsule constituents and methods should be devised for increasing the cooling capability of the unit and for reducing or overcoming the accelerations produced by spin.</p>					
17. KEY WORDS			18. DISTRIBUTION STATEMENT Unclassified - unlimited  <i>A. C. Yates</i>		
19. SECURITY CLASSIF. (of this report) Unclassified		20. SECURITY CLASSIF. (of this page) Unclassified		21. NO. OF PAGES 66	22. PRICE NTIS

# TABLE OF CONTENTS

	Page
INTRODUCTION .....	1
DESCRIPTION .....	3
Vehicles .....	3
Aerobee 170A Research Rocket and the Flight of NASA 13.113 .....	3
Black Brank VC Research and the Flight of NASA 21.006 .....	14
Experiment .....	17
Temperature Control Unit, Zero-g Experiment, Aerobee Rocket, MIT 15473 .....	17
Integration of Units into Research Rockets .....	17
Flight Data .....	27
Aerobee 170A Research Rocket and the Flight of NASA 13.113 .....	27
Capsule .....	31
Objective .....	31
Description of Sample .....	31
Preparation and Processing of Sample .....	31
Evaluation of Sample .....	42
CONCLUSIONS .....	56
RECOMMENDATIONS .....	58
APPENDIX — AEROBEE 170 VIBRATION SPECIFICATION .....	59

# LIST OF ILLUSTRATIONS

Figure	Title	Page
1.	Aerobee 170A Research Rocket on a Nike launcher . . . . .	4
2.	Altitude versus time for Aerobee 170A NASA 13.113 . . . . .	5
3.	Aerobee 170A NASA 13.113 configuration . . . . .	7
4.	Relationships between spin rate, coning (precession) angle and rate, and nutation before and after yo-yo despin of Aerobee 170A NASA 13.113 . . . . .	9
5.	Black Brant VC Research Rocket . . . . .	15
6.	Temperature Control Unit, Zero-g Experiment, Aerobee Rocket, MIT 15473 . . . . .	18
7.	Cross section of Temperature Control Unit, Zero-g Experiment Aerobee Rocket, MIT 15473, with major components labeled . . . . .	19
8.	Oblique view of Unit mounted in 0.38 m (15 in.) long cylindrical section of an Aerobee 170A Research Rocket . . . . .	20
9.	Top view of Unit mounted in 0.38 m (15 in.) diameter cylindrical section of an Aerobee 170A Research Rocket . . . . .	21
10.	Unit mounted in a section of Black Brant VC Research Rocket NASA 21.006 . . . . .	22
11.	Test setup used to obtain time-temperature curves with capsule containing InBi and a thermocouple located at its center in the Unit . . . . .	24
12.	Time versus temperature relationship developed by MSFC for processing capsule on Aerobee 170A NASA 13.113 . . . . .	25



## LIST OF ILLUSTRATIONS (Continued)

Figure	Title	Page
13.	Time versus temperature relationship developed by MSFC for processing capsule on Black Brant VC NASA 21.006 . . . . .	26
14.	Altitude versus time for Aerobee 170A NASA 13.113 and temperature versus time for Temperature Control Unit . . . . .	28
15.	Acceleration at inner wall of capsule produced by spinning and coning of Aerobee 170A NASA 13.113 . . . . .	29
16.	Sample configuration . . . . .	32
17.	Casting of layup wires — molten InBi injected in 0.76 m (30 in.) long plastic tube 0.001 m (0.045 in.) in diameter containing 4 Cu-Be wires 0.001 m (0.005 in.) in diameter . . . . .	33
18.	Layup at various stages of assembly and layup tooling . . . . .	34
19.	Layup in press for bonding . . . . .	35
20.	Cutting of layup disks — first layup . . . . .	36
21.	Layup cells . . . . .	37
22.	Coin tooling . . . . .	38
23.	Tooling for coins in press . . . . .	39
24.	Finished coin . . . . .	40
25.	Argon filled chamber used for sample assembly . . . . .	41
26.	Section of B sample . . . . .	42
27.	A sample half as removed from capsule . . . . .	43

## LIST OF ILLUSTRATIONS (Continued)

Figure	Title	Page
28.	B sample half, external surface as removed from capsule . . . . .	45
29.	B sample, longitudinal sections as sectioned . . . . .	46
30.	Transverse section of ground control sample . . . . .	47
31.	Longitudinal section of ground control sample . . . . .	47
32.	Longitudinal section of flight sample VI/IF-B . . . . .	48
33.	Longitudinal section of flight sample VI/IF-A . . . . .	48
34.	Longitudinal section VI/IF-B showing etched macrostructure of Aerobee wafer composite . . . . .	49
35.	Microstructure at Area 1, Figure 34 . . . . .	50
36.	Microstructure in melted area at Area 2, Figure 34 . . . . .	50
37.	Duplex microstructure in transition zone at Area 3, Figure 34 . . . . .	51
38.	Unaffected microstructure at Area 4, Figure 34 . . . . .	51
39.	Surface view of as-received wafer showing macrostructure and configuration of bubbles . . . . .	52
40.	Surface at periphery of as-received wafer . . . . .	53
41.	Surface microstructure between bubbles near center of as-received wafer . . . . .	53

## LIST OF ILLUSTRATIONS (Concluded)

Figure	Title	Page
42.	Transverse section exhibiting macrostructure of disk number 3 near bottom of composite . . . . .	54
43.	Enlargement of area at black circle showing recrystallized structure in melted areas . . . . .	54
44.	Enlargement of area at rectangle exhibiting microstructure of transition area between melted and unaffected structure . . . . .	55
45.	Enlargement of area at white circle depicting unaffected structure . . . . .	55

RESEARCH ROCKET TESTS RR-1 (BLACK BRANT VC)  
AND RR-2 (AEROBEE 170A): INVESTIGATIONS OF  
THE STABILITY OF BUBBLES IN PLAIN  
AND FIBER-REINFORCED METAL MELTED  
AND SOLIDIFIED IN A NEAR-ZERO-g ENVIRONMENT

INTRODUCTION

In the Spring of 1966, Mr. Hans Wuenscher<sup>1</sup> conceived the idea of processing materials in the weightless environment of space with the goal of obtaining materials with improved or unique mechanical, electrical, and/or optical properties.

In December 1969, he conceived the idea of placing experiments on Apollo 14 to demonstrate that materials with unique properties can be made in a weightless environment. These experiments were later named the Apollo 14 Flyback Composite Casting Demonstrations. Eleven of the 14 capsules prepared for Apollo 14 were processed by the crew. The results of these demonstrations are discussed in a Marshall Space Flight Center (MSFC) document, S&E-PT-IN-71-1, dated July 13, 1971.

While attending the International Solar Society's Solar Energy Conference at NASA's Goddard Space Flight Center (GSFC) in May 1971, Mr. Wuenscher visited the Sounding Rocket Division to determine the availability of space on sounding rockets for processing materials. He found that many rockets flown have some lead ballast which could be exchanged for another experiment.

---

1. Assistant Director for Advanced Projects, Process Engineering Laboratory, MSFC.

In June 1971, Mr. Wuenschel, Mr. John Ransburgh<sup>2</sup>, and Mr. Vaughn Yost<sup>3</sup> visited GSFC to discuss with Mr. Robert Pincus<sup>4</sup> and Mr. Morgan Windsor<sup>5</sup> the possibility of putting an experiment containing an unused Apollo Flyback capsule on an Aerobee 170A rocket, designated NASA 13.113, which was to be launched from U. S. Navy Ordnance and Missile Test Facility (USNOMTF) at White Sands, New Mexico.

Mr. Yost was named Project Engineer and Mr. Ransburgh's unit was given responsibility for designing the Temperature Control Unit, Zero-g Experiment Aerobee, MIT 15473 (Unit); Mr. John White of that group designed the Unit. Mr. Isaac Edmond, Jr.<sup>6</sup>, oversaw the manufacture and assembly of the Unit, conducted all functional tests, and conducted all the time-temperature tests to obtain the time-lines for not only the Aerobee flight but also flight on a Black Brant VC rocket. Mr. Garland Johnston<sup>7</sup> conducted the dynamic tests per the Aerobee 170 Vibration Specification (see the Appendix).

The objectives of this series of research rocket experiments were (1) to learn about the capabilities of these rockets, (2) to learn how to interface the payloads and rockets (e.g., the prime mechanical interface is a bolt circle; other interfaces are power, timers, and telemetry), and (3) to process some of the composite casting demonstration capsules intended originally for Apollo 15.

On October 19, 1971, GSFC's Aerobee 170A NASA 13.113 was successfully launched and recovered at the USNOMTF. All of the objectives were met.

On January 27, 1972, GSFC's Black Brant VC NASA 21.006 was successfully launched from NASA's Wallops Island, Virginia. Telemetry signals from this vehicle indicated that the squibbs which separate the heat shield from the payload were not ignited and the payload was lost.

This report contains the results of the Aerobee flight as well as data on the Aerobee 170A and Black Brant VC rockets.

- 
2. Tool Design Branch, Process Engineering Laboratory, MSFC.
  3. Chief, Metals Processing Section, Process Engineering Laboratory, MSFC.
  4. Chief, Payload Design Section, Sounding Rocket Division, GSFC.
  5. Payload Design Section, Sounding Rocket Division, GSFC.
  6. Metal Processing Section, Process Engineering Laboratory, MSFC.
  7. Vibration and Acoustics Test Section, Astronautics Laboratory, MSFC.

# DESCRIPTION

## Vehicles

### AEROBEE 170A RESEARCH ROCKET AND THE FLIGHT OF NASA 13.113

This vehicle (Fig. 1) is manufactured by the Space General Division of Aerojet General Corporation, El Monte, California. It can be launched from the Nike launcher (Fig. 1), the multiple-purpose launcher, or the adjustable Aerobee towers at NASA's facilities at Wallops Island, Virginia and USNOMTF at White Sands, New Mexico.

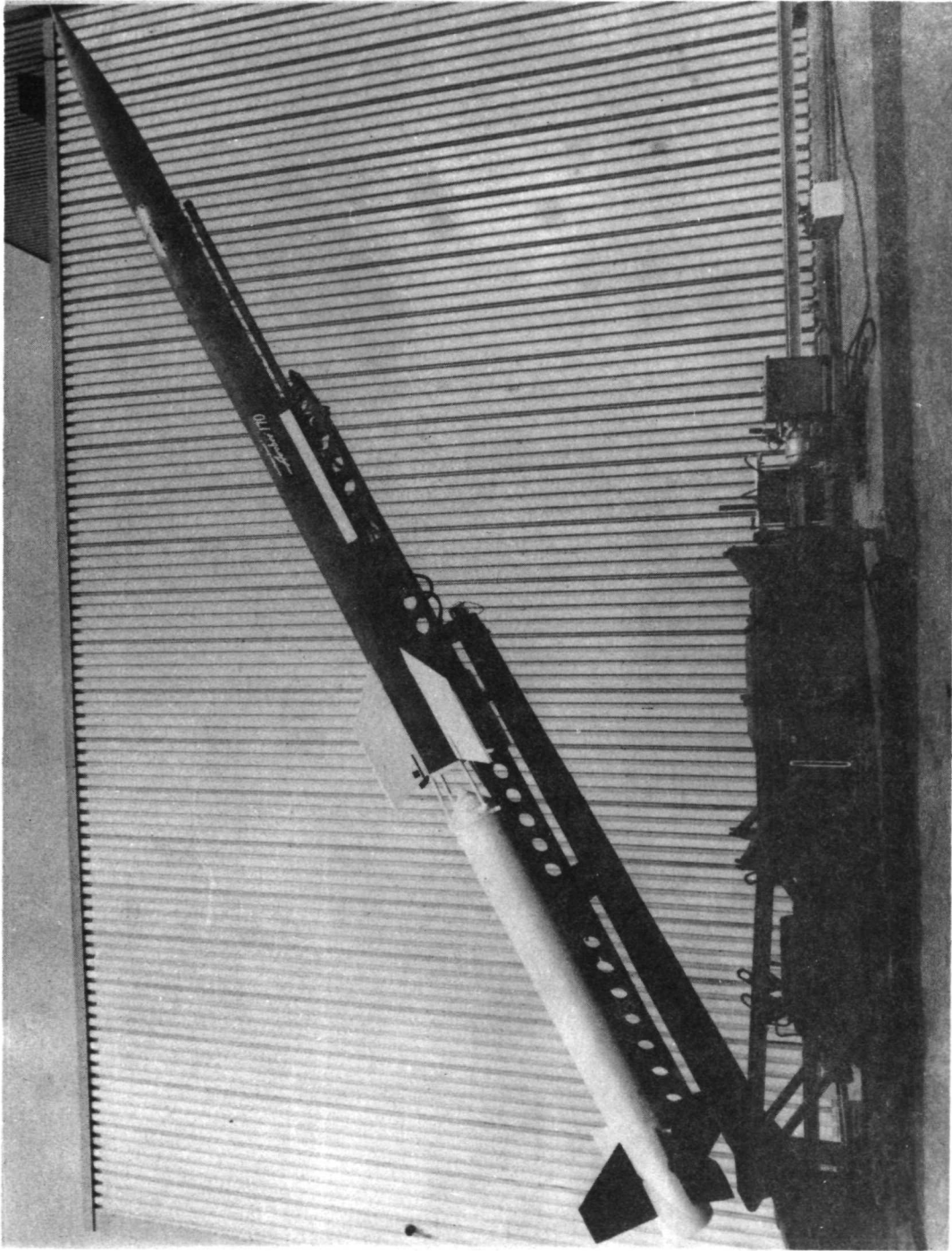
Aerobee 170A NASA 13.113 was flown from Aerobee 150 tower B at the USNOMTF. This flight was launched at 11:30 a.m., MDT, on October 19, 1971. Although the vehicle carried some science and rocket engineering instrumentation, it was primarily a test round to aid in evaluating the dispersion characteristics of this three-finned version of the Aerobee 170. The meteorological report<sup>8</sup> on this launch revealed a theoretical apogee altitude of 155.00 km (96.4 mi) and a theoretical impact point 97.17 km (60.7 mi) north and 7.40 km (4.6 mi) west of the launcher. The actual apogee was 147.22 km (91.5 mi) and an impact point was 91.33 km (58.3 mi) north and 2.41 km (1.5 mi) west of the launcher (Fig. 2)

The Aerobee 170A is composed of a three-fin Aerobee 150A sustainer and the Nike booster system. The solid propellant booster and liquid propellant sustainer are fired simultaneously with the sustainer ignition controlled by the standard start valve and burst diaphragms. At booster ignition, the sustainer is pressurized and starts to thrust at 0.6 sec. The booster drag separates at 3.35 sec.

This rocket had an outside diameter of 0.38 m (15 in.) and a length of approximately 12.89 m (507.48 in.), of which 3.88 m (152.75 in.) was the sustainer and 4.05 m (159.31 in.) was the payload for Aerobee 170A NASA 13.113. The overall length of NASA 13.113 was 16.49 m (636.79 in.). The vehicle trajectory is dependent on the effective launch angle and the mass of the payload. The mass of NASA 13.113 was 422.92 kg (3137 lbm) at lift-off, of which 202.07 kg (445.5 lbm) was payload. After burnout, 51.27 sec into the flight, its total mass was 349.1 kg (748.1 lbm). A number of channels of telemetry are usually available for transmitting rocket and payload data to the ground.

---

8. Prepared by the Atmospheric Sciences Laboratory, White Sands Missile Range.



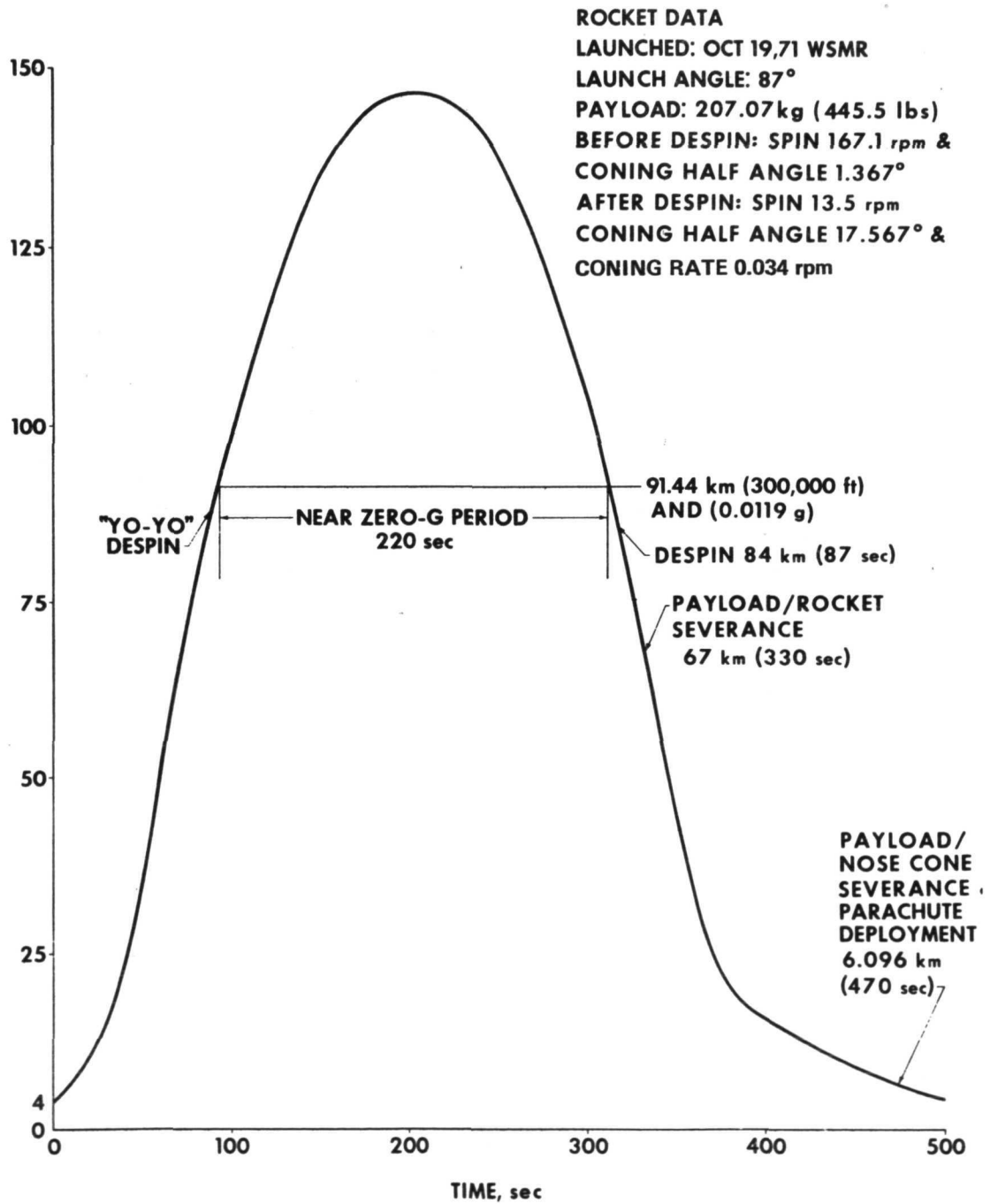


Figure 2. Altitude versus time for Aerobee 170A NASA 13.113.



Mr. Roy McIntosh, Jr.,<sup>9</sup> the other experimenter on Aerobee 170A NASA 13.113, had two Endevco Q-Flex low level accelerometers in his experiment area. One, on telemetry channel 13, was mounted in a plane parallel to the long axis of the rocket to measure thrust levels and the other, on telemetry channel 15, in a plane perpendicular to the long axis to measure angular accelerations. Both were mounted  $0.127 \pm 0.0127$  m ( $5 \pm 1/2$  in.) from the long axis of the vehicle and  $2.413 \pm 0.0127$  m ( $95 \pm 1/2$  in.) from its tip. After burnout, the center of gravity of the vehicle was 4.11 m (162.1 in.) from its tip or 1.711 m (67.1 in.) aft of the accelerometers (Fig. 3).

The vehicle can be despun with a "yo-yo" despin system. Yo-yo despin is accomplished by deploying weights on the ends of cables which are attached to the vehicle. Two cable and weight assemblies are used. The vehicle can be despun with this system to approximately any desired rate including zero by selecting appropriate cable lengths and weight masses.

The trajectory profile for NASA 13.113 is shown in Figure 2. Yo-yo despin occurred between 83.2661 and 83.3662 sec,<sup>10</sup> according to the spin accelerometer which showed a change in acceleration of  $-0.10$  to  $-0.052$  g. This is confirmed by the thrust accelerometer which showed a deceleration of  $+0.108$  to  $+0.044$  g between 83.3662 and 83.4668 sec.<sup>11</sup>

After 85.8780 sec, the spin accelerometer reached a mean acceleration of  $-0.026$  g. From this, the spin rate after despin was calculated to be approximately 13.52 revolutions per min, as shown below

$$a_R = r \omega^2 \quad , \quad \omega^2 = \frac{a_R}{r} \quad (1)$$

---

9. Thermophysics Branch, Engineering Physics Division, Space Applications and Technology Directorate, GSFC.

10. Spin accelerometer, Aerobee 170A NASA 13.113 telemetry channel 15 (2251.5 Mhz) Time versus TM volts.

11. Thrust accelerometer, Aerobee 170A NASA 13.113 telemetry channel : (2251.5 Mhz) Time versus TM volts.

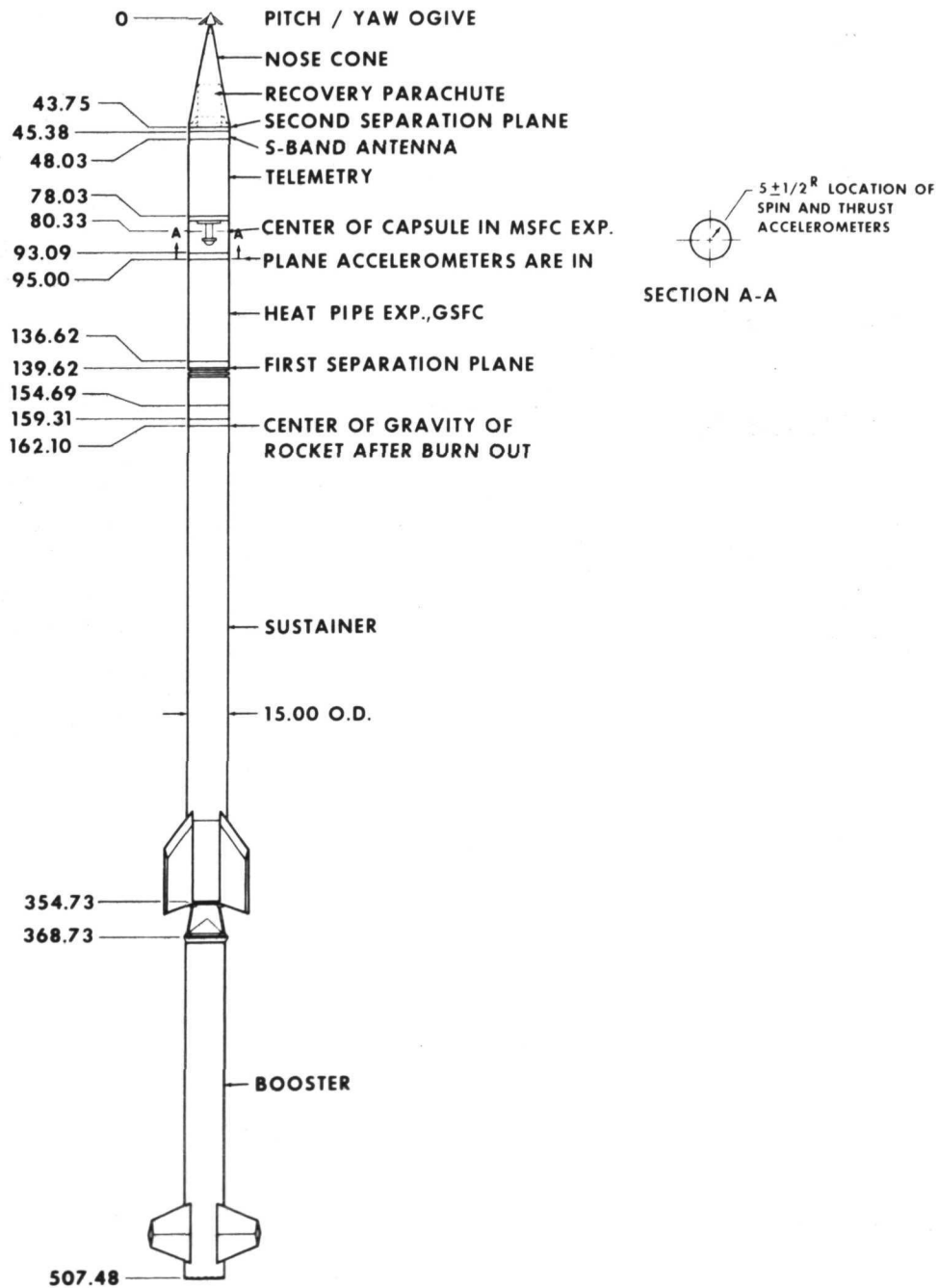


Figure 3. Aerobee 170A NASA 13.113 configuration.

where

$a_R$  radial component of acceleration, in  $m/sec^2$  ( $ft/sec^2$ )

$r$  radius, here the distance of the spin accelerometer from the spin axis of the vehicle, in m (in.)

$\omega'$  angular velocity of the vehicle, in radians/sec

$$\omega'^2 = \frac{(0.026 \text{ g} \times 9.81) m/sec^2}{0.127 \text{ m}}$$

$$\omega'^2 = 2.008 / sec^2$$

$$\omega' = 1.417 \text{ rad/sec}$$

and

$$n' = \frac{2\pi \omega'}{60} \tag{2}$$

where

$n'$  angular velocity, in revolutions per minute

$$n' = 1.417 \text{ rad/sec} \times \frac{1 \text{ rev}}{2\pi \text{ rad}} \times \frac{60 \text{ sec}}{\text{min}} = 13.52 \text{ rpm}$$

Generally, at low atmospheric pressures (3.7 microns Hg) at 84 m (52.21 mi) where despin occurs, as the spin rate decreases, precession about the center of gravity of the vehicle [called coning (Figs. 4a and 4b) in research vehicles] increases. With precession, an up and down oscillation of the vehicle axis [called nutation (Fig. 4c)] occurs. The latter is caused

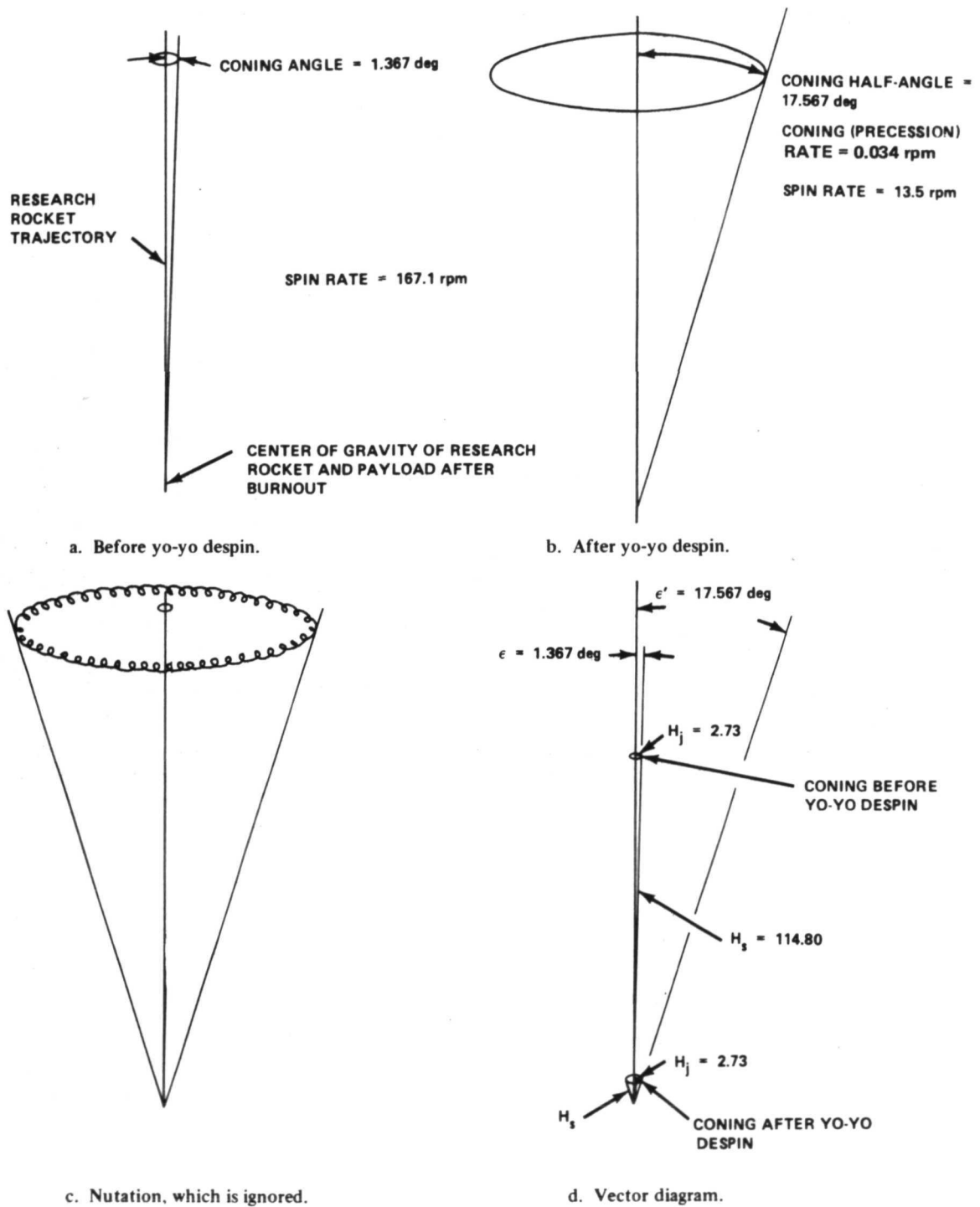


Figure 4. Relationships between spin rate, coning (precession) angle and rate, and nutation before and after yo-yo despin of Aerobee 170A NASA 13.113.

by things such as mass asymmetries but is very small in amplitude and may be ignored. The angle  $\epsilon$  is defined as the coning half-angle and, assuming no external forces act on the vehicle, this angle remains constant. The magnitude of this angle is defined by the ratio between the vehicle angular momentum in the pitch/yaw and the spin planes. If this relationship changes, the magnitude of the coning angle also changes. In the case of vehicle despin, the spin momentum is suddenly reduced and the coning angle is consequently increased. This situation is illustrated in Figure 4d.

The relationship between the spin and pitch/yaw angular momenta prior to despin is given by

$$H = \sqrt{H_s^2 + H_j^2} \quad (3)$$

also

$$\tan \epsilon = \frac{H_j}{H_s} \quad (4)$$

where

$H$  total momentum of the vehicle, in  $\text{kg}\cdot\text{m}^2/\text{sec}$  ( $\text{slug}\cdot\text{ft}^2/\text{sec}$ )

$H_s$  spin angular momentum prior to despin, in  $\text{kg}\cdot\text{m}^2/\text{sec}$  ( $\text{slug}\cdot\text{ft}^2/\text{sec}$ )

$H_j$  pitch/yaw angular momentum prior to despin, in  $\text{kg}\cdot\text{m}^2/\text{sec}$  ( $\text{slug}\cdot\text{ft}^2/\text{sec}$ )

$\epsilon$  coning half-angle prior to despin, in degrees

After despin, the spin momentum is reduced to  $H_s'$ , but the pitch/yaw momentum remains unchanged. The new coning angle is given by

$$\tan \epsilon = \frac{H_j}{H_s'} \quad (5)$$

where

$H_S$  spin angular momentum after despin, in kg-m<sup>2</sup>/sec  
(slug-ft<sup>2</sup>/sec)

$\epsilon'$  coning half-angle after despin, in degrees

Comparing equations (4) and (5) yields

$$H_S \tan \epsilon = H'_S \tan \epsilon'$$

$$\tan \epsilon' = \frac{H_S}{H'_S} \tan \epsilon \quad (6)$$

The spin angular momentum is also the spin moment of inertia times the spin rate. Hence,

$$H_S = I_S \omega \quad (7)$$

and

$$H'_S = I_S \omega' \quad (8)$$

where

$I_S$  spin moment of inertia of the vehicle, in kg-m<sup>2</sup> (slug-ft<sup>2</sup>)

$\omega$  spin rate prior to despin, in radians/sec

$\omega'$  spin rate after despin, in radians/sec

Substituting equations (7) and (8) into equation (6) yields

$$\tan \epsilon' = \frac{\omega}{\omega'} \tan \epsilon \quad (9)$$

It is also noted that not only does the coning angle change, but the fixed line in space about which the vehicle cones also changes. This is seen in Figure 4c.<sup>12</sup>

The coning rate is the angular rate at which the vehicle describes the cone and is given by

$$\sigma = \omega' \frac{I_s}{I_j} \frac{\cos \alpha}{\cos \epsilon'} \quad (10)$$

where

$\sigma$  coning rate, in radians/sec

$I_j$  pitch/yaw moment of inertia of the vehicle, in kg-m<sup>2</sup> (slug-ft<sup>2</sup>)

$I_s$  spin moment of inertia of the vehicle, in kg-m<sup>2</sup> (slug-ft<sup>2</sup>)

$\omega'$  spin rate after despin, in radians/sec

$\epsilon'$  coning half-angle after despin, in degrees<sup>13</sup>

From this, the coning half-angle before and after yo-yo despin, as well as the coning rate for NASA 13.113, were calculated to be approximately 1.367 deg, 17.567 deg, and 0.034 rpm, respectively.

Coning Half-Angle Before Yo-Yo Despin. Between 81 and 90 sec into the rocket's trajectory, its pitch/yaw angle,  $\omega_j$ , changed from 8.01 to 8.58 deg, or

$$\frac{\frac{8.58 \text{ deg} - 8.01 \text{ deg}}{9 \text{ sec}}}{57.2958 \text{ deg/rad}} = \frac{0.0633 \text{ deg/sec}}{57.2958 \text{ deg/rad}} = 0.0011 \text{ rad/sec}$$

12. Letter No. 600-00-2 dated November 8, 1971, from B. R. Payne, Design Engineer, Rocket and Space Division, Bristol Aerospace (1968) Limited, P.O. Box 874, Winnipeg, Canada.

13. S.W. Groesberg, Advanced Mechanics, John Wiley & Sons, Inc., New York, 1968, pp. 195-198.

$$\tan \epsilon = \frac{H_j}{H_s} = \frac{I_j \omega_j}{I_s \omega_s} = \frac{2484 \text{ slug-ft}^2 \times 0.0011 \text{ rad/sec}}{6.56 \text{ slug-ft}^2 \times 17.5 \text{ rad/sec}} = \frac{2.7324}{114.80}$$

$$\tan \epsilon = 0.0238$$

$$\epsilon = \arctan 0.0238 = 1.367 \text{ deg}$$

#### Coning Half-Angle After Yo-Yo Despin.

$$\tan \epsilon' = \frac{H_j}{H_s'} = \frac{2.7324}{6.56 \text{ slug-ft}^2 \times 1.38 \text{ rad/sec}} = \frac{2.7324}{9.05}$$

$$\tan \epsilon' = 0.3019$$

$$\epsilon' = \arctan 0.3019 = 17.567 \text{ deg}$$

#### Coning Rate.

$$\sigma = \omega' \frac{I_s \cos \alpha}{I_j \cos \epsilon'} = \frac{1.417 \text{ rad/sec} \times 6.56 \text{ slug-ft}^2 \times \cos 17.567^\circ}{2484 \text{ slug-ft}^2 \times \cos 1.367^\circ}$$

$$\sigma = \frac{1.417 \times 6.56 \times 0.9532}{2484 \times 0.9997} = 0.00357 \text{ rad/sec}$$

$$\sigma = 0.00357 \text{ rad/sec} \times \frac{60 \text{ sec}}{\text{min}} \times \frac{\text{rev}}{2\pi} = 0.034 \text{ rpm}$$

Space General also makes the Mark II Attitude Control System which is a multiple-purpose system for exo-atmospheric attitude control of rocket payloads. It is inertially referenced and provides three-axis control of the payload by use of cold gas reaction jets. Preprogrammed guidance data sequences control the payload attitude. This was not used on NASA 13.113.

On payloads with experiments that are forward looking, e.g., photographing celestial bodies, the nose cone is severed from the rocket/payload on the upward leg of the flight. Generally, when the payload does not contain



a forward looking experiment, the nose cone is not severed until late in the flight. On NASA 13.113 both severances occurred on the downward leg of the flight because there were no forward looking experiments on it. The first severance, ( Figs. 2 and 3) payload from the rocket, occurred at an altitude of approximately 67 km (41.63 mi) between 329.7740 and 331.9840 sec according to the spin accelerometer and between 329.7740 and 330.4768 sec according to the thrust accelerometer into the flight.

The second severance, ( Figs. 2 and 3) nose cone from payload, was actuated by an aneroid switch set for 6.096 km (3.79 mi). This severance occurred approximately 470 sec into the flight.

After the payload enters the atmosphere, it makes a difference whether the nose cone has been severed or not. If the payload has the nose cone off, the payload will come down a flat spin with the forward edge of the plane of spin tilted up 20 to 30 deg with respect to the surface of the impact area. If the nose cone is left on, as in the case NASA 13.113, the payload/nose cone will tend to come down nose first.

The parachute may be attached to either the forward or aft end of the payload. Of course, with forward looking experiments in the payload, it must be attached to the aft end. On NASA 13.113 it was attached to the forward end of the payload and the severed nose cone was used to pull its rip cord and pull the parachute from its canvas pack.

#### BLACK BRANT VC RESEARCH AND THE FLIGHT OF NASA 21.006

The vehicle ( Fig. 5) is manufactured by Bristol Aerospace (1968) Limited, Winnipeg, Canada. It can be launched from the adjustable Aerobee towers at Wallops Island and White Sands.

Black Brant VC NASA 21.006 was flown from the Aerobee tower on Wallops Island. This flight was launched at 11:30 a. m., EST, on January 27, 1972. Although this vehicle carried an MSFC experiment, it was, primarily, a test round to verify the Black Brant VC system.

The Black Brant V has a single stage solid propellant motor. The "C" model is fitted with four fins which can be set to produce the required spin (roll) rate. This rocket has an outside diameter of 0.43 m (17.2 in.) and a length of 5.27 m (207.61 in.) plus the payload, which was 3.50 m (134.87 in.) at launch for NASA 21.006. After the payload was severed from the rocket, the payload was 3.16 m (124.45 in.) long because severance occurred

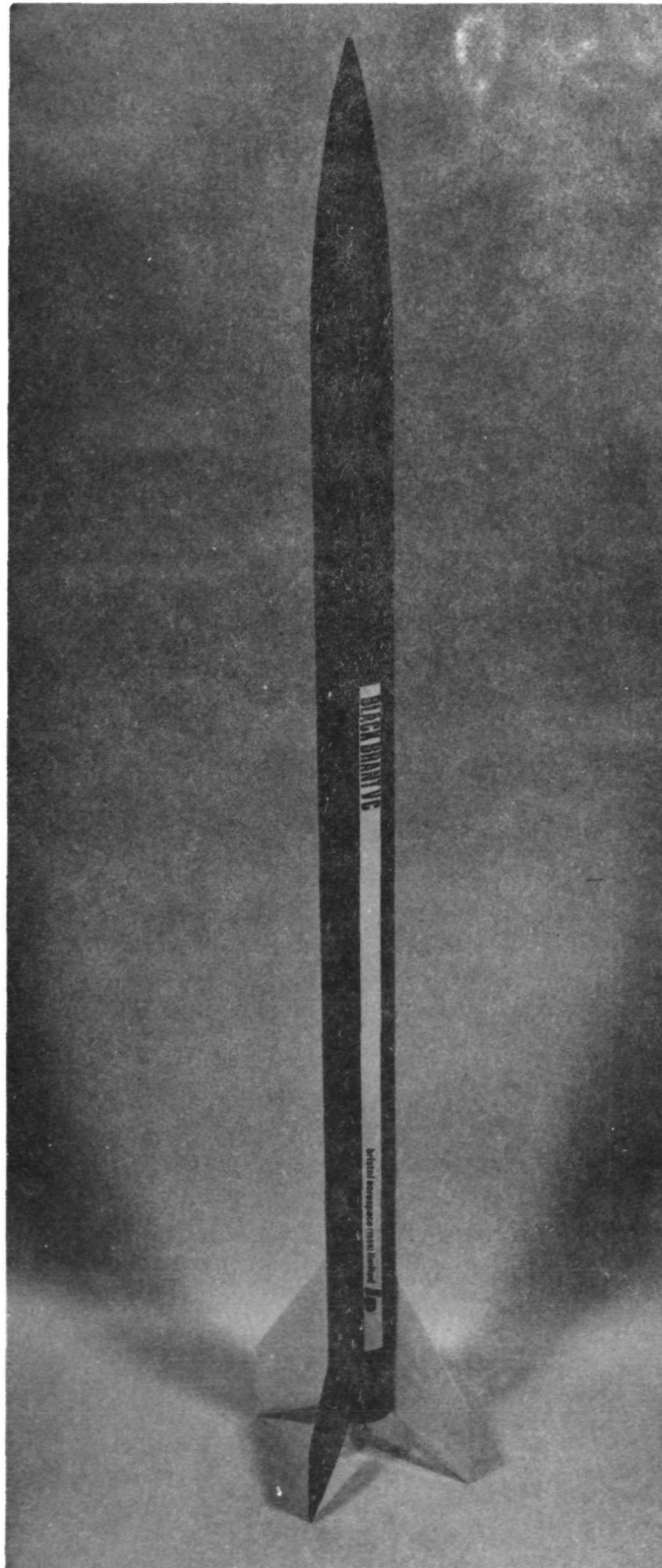


Figure 5. Black Brant VC Research Rocket.

0.25 m (10.42 in.) forward of the aft end of the payload. The overall length of NASA 21.006 was 8.71 m (342.48 in.).

The Black Brant VC trajectory is dependent on the effective launch angle and the mass of the payload. The angle of launch was 80 deg but, when the effect of the winds was taken into consideration, the effective angle of launch was 80.7 deg. The mass of NASA 21.006 was 1261.89 kg (2782 lbm) at lift-off, of which 256.73 kg (566 lbm) was payload. After burnout, the mass of the vehicle was 501.22 kg (1105 lbm), of which 244.49 kg (539 lbm) was the rocket. The trajectory was calculated to have an altitude of 240.32 km (149.33 mi) and a range of 192.50 km (119.62 mi). Radar used to track this vehicle indicated that actual altitude and range were 221.47 km (141.97 mi) and 251.46 km (156.25 mi), respectively.

Since this was a test round, the major events of the flight were monitored and the data telemetered to the ground. These data were recorded on strip charts. These charts indicated the despin occurred at 55 sec and the spin rates before and after despin were 4.10 rps and 1.95 rps, respectively. The desired rate after despin was 1.00 rps. Other charts indicated that the payload/nose cone was severed from the rocket at 60 sec and that the flight was a success up to the point where the heat shield was suppose to be severed from the aft end of the payload at 6.10 km (3.79 mi). According to this chart severance did not occur. Radar tracking ceased at approximately 4.87 km (3.03 mi) above sea level because of the curvature of the earth and the fact that radar signals bend only slightly. However, between 4.87 km (3.03 mi) and 6.10 km (3.79 mi) there was no indication on the radar that the heat shield was severed from the payload or that the parachute was deployed.

A four engine plane was flown to the point of impact but neither the dye marker nor the payload was found. For this reason and the fact that 241.15 km (150 mi) is about the maximum range of the helicopters, they were never sent out. The following day the weather was too bad to send out the airplane. However, the U.S. Navy sent one of its newest submarines to the impact area to search the area and bottom with sonar. The water was about 3.1 km (1700 fathoms) at the point of impact. The impact area was searched the next day with the airplane. The payload was not found and is most likely lost because Wallops Station has never had a payload sighted or recovered by a passing ship.

## Experiment

### TEMPERATURE CONTROL UNIT, ZERO-g EXPERIMENT, AEROBEE ROCKET, MIT 15473

This Unit (Fig. 6) was developed to verify and complete the Apollo Flyback Composite Casting Demonstrations with research rockets such as the Aerobees and Black Brants. Briefly, this is accomplished by heating the contents of the capsules so the phase change from solid to liquid occurs in near-zero-g (above 91.44 km or 56.82 mi)<sup>14</sup>, keeping the contents liquid to permit the occurrence of any changes, and then cooling the capsule to produce a change in phase from liquid to solid before leaving near-zero-g.

### Integration of Units into Research Rockets

The major components are noted on the cross section of the Unit shown in Figure 7.

Integration of a Unit into a rocket includes the following: disassembling the Unit sufficiently to insert the flight capsule in the heater and reassemble; filling the hemispherical dome with water; mechanically attaching the Unit mounting plate to the bolt circle in the rocket section; charging the battery pack; installing the battery pack in the rocket section; electrically connecting heater and solenoid relays to the timers, battery pack, and Unit; setting the timers; and verifying that the system is operational.

A Unit is shown mounted in a 0.38 m (15 in.) long cylindrical section of an Aerobee 170A (Figs. 8 and 9). Figure 10 shows another Unit mounted in a section of a Black Brant VC.

For both rockets, the Unit was mounted so the centerlines of the vehicle and Unit are coincidental to reduce the effect of centrifugal forces on the capsule contents produced by spinning and coning .

---

14. Letter dated October 14, 1971, from J. N. Brown, Advanced Programs, Space General Division, Aerojet General Corporation, El Monte, CA 91734.

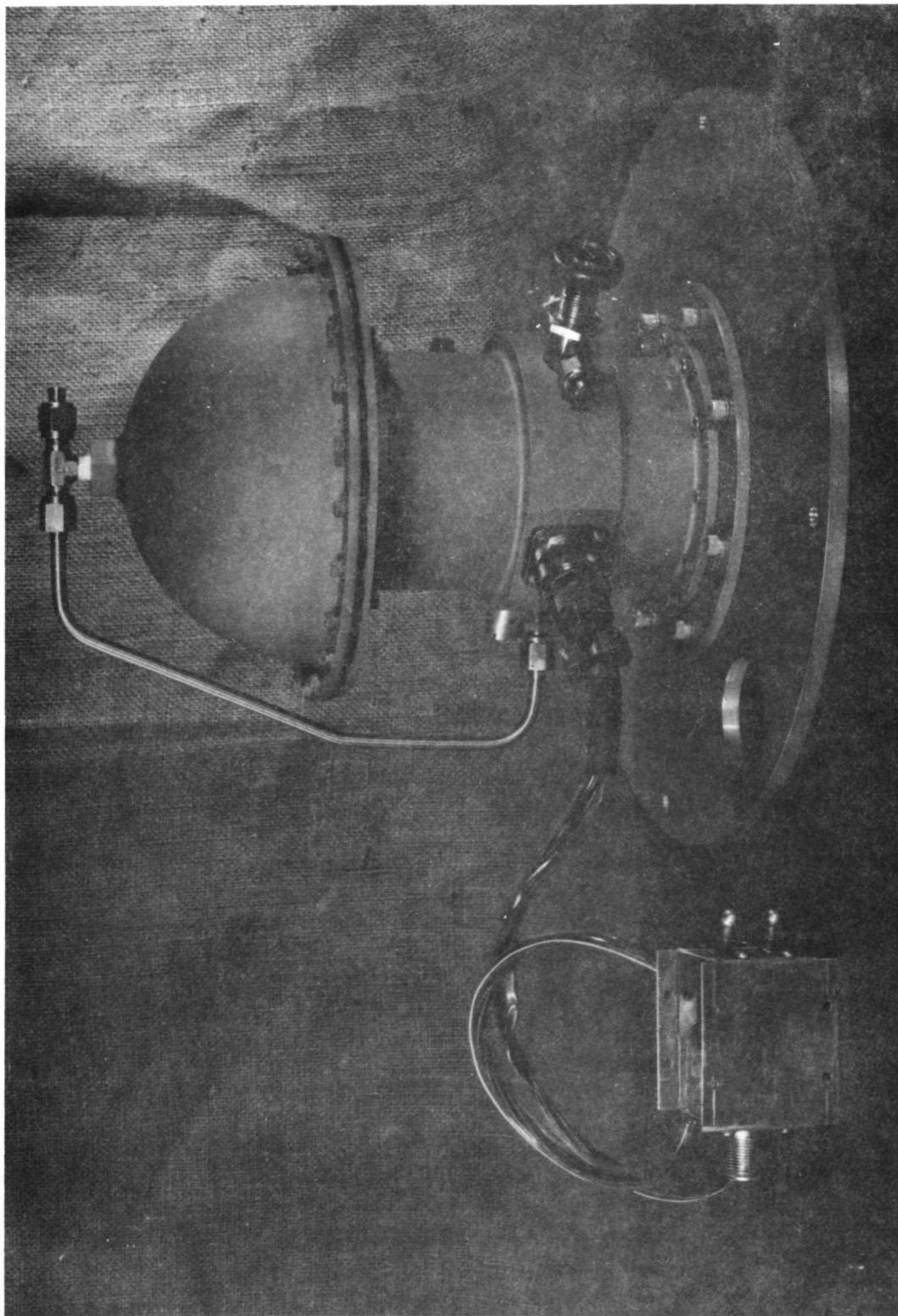


Figure 6. Temperature Control Unit, Zero-g Experiment, Aerobee Rocket, MIT 15473.

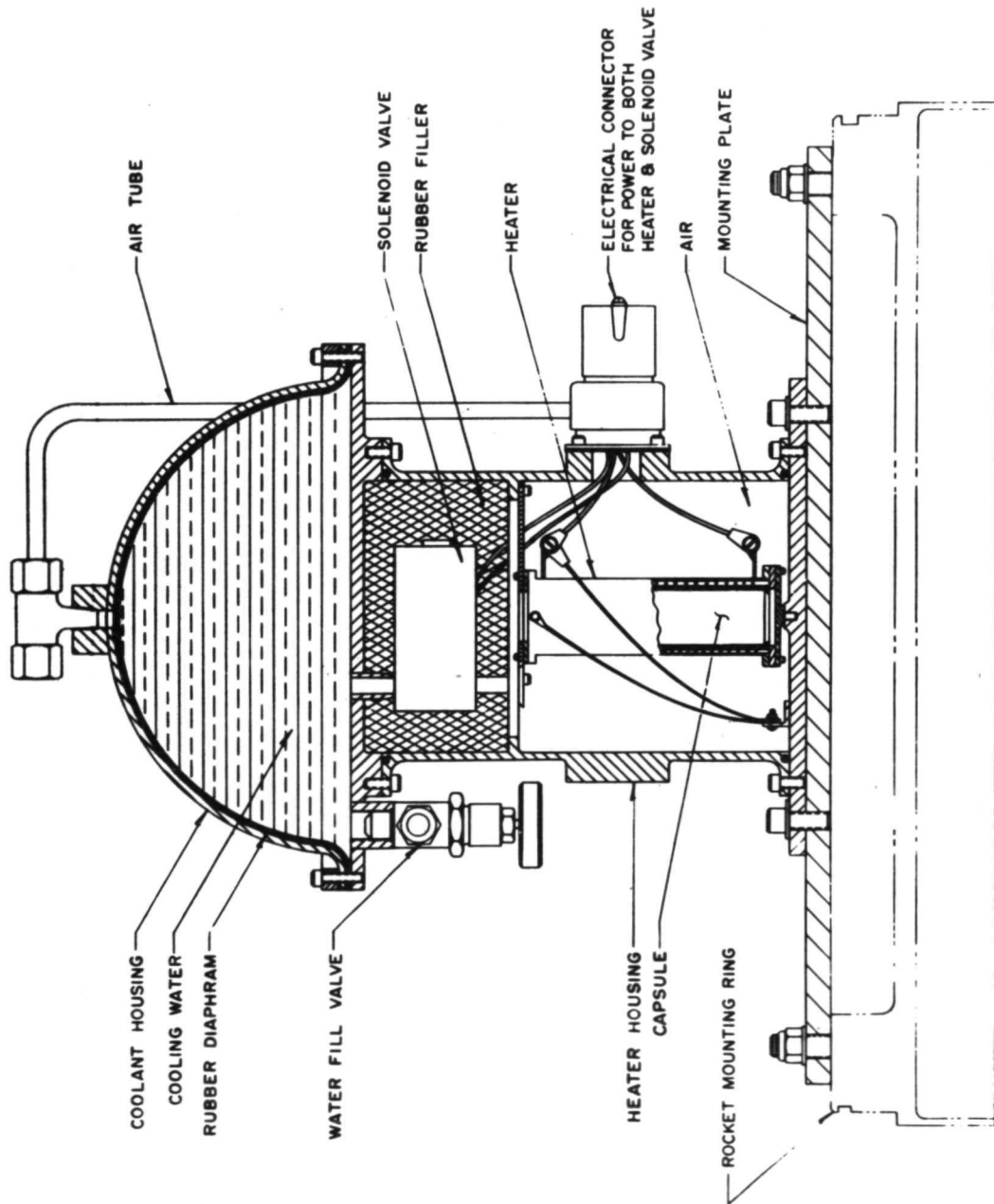


Figure 7. Cross section of Temperature Control Unit, Zero-g Experiment Aerobee Rocket, MIT 15473, with major components labeled.

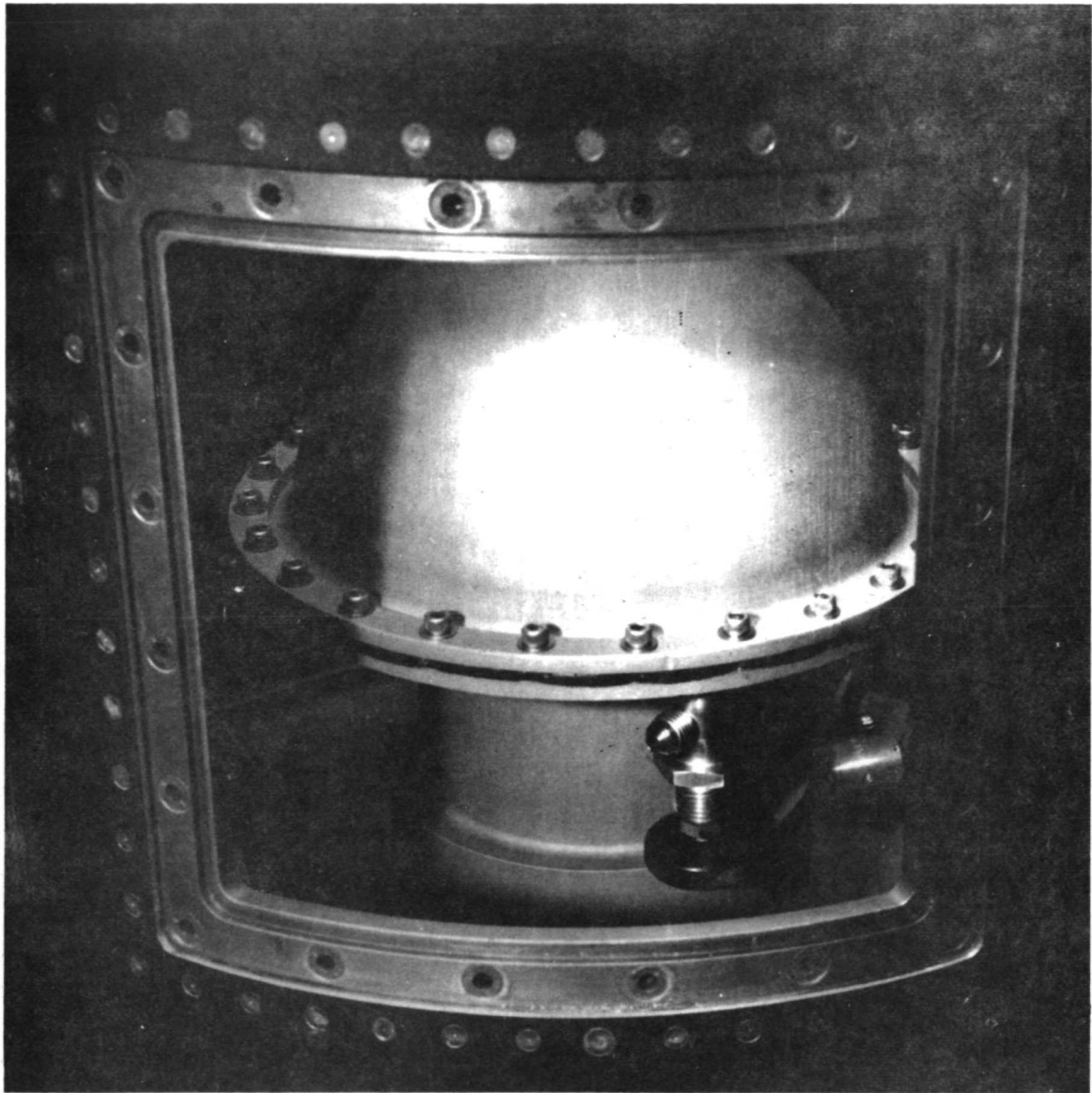


Figure 8. Oblique view of Unit mounted in 0.38 m (15 in.) long cylindrical section of an Aerobee 170A Research Rocket.



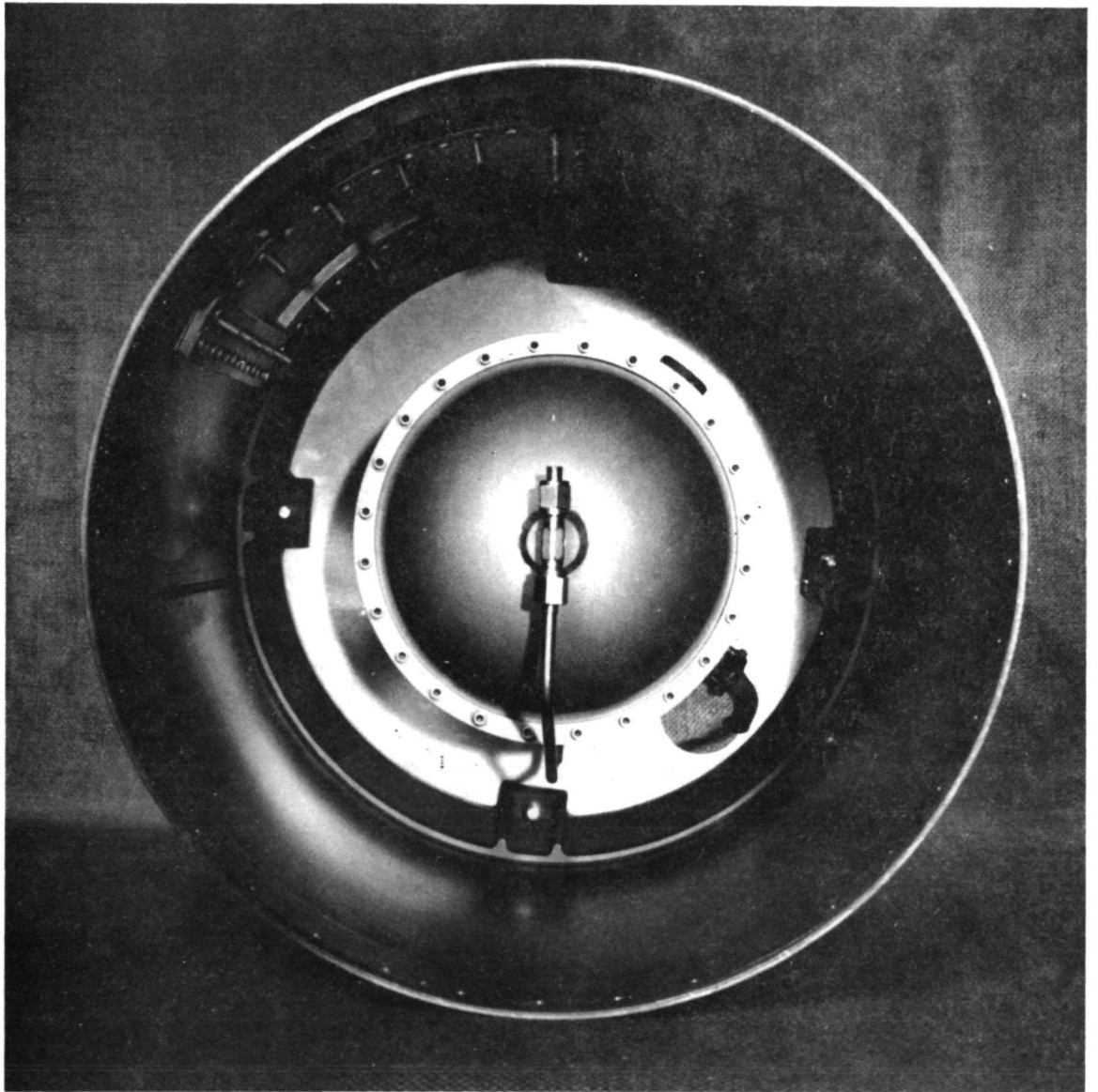


Figure 9. Top view of Unit mounted in 0.38 m (15 in.) diameter cylindrical section of an Aerobee 170A Research Rocket.



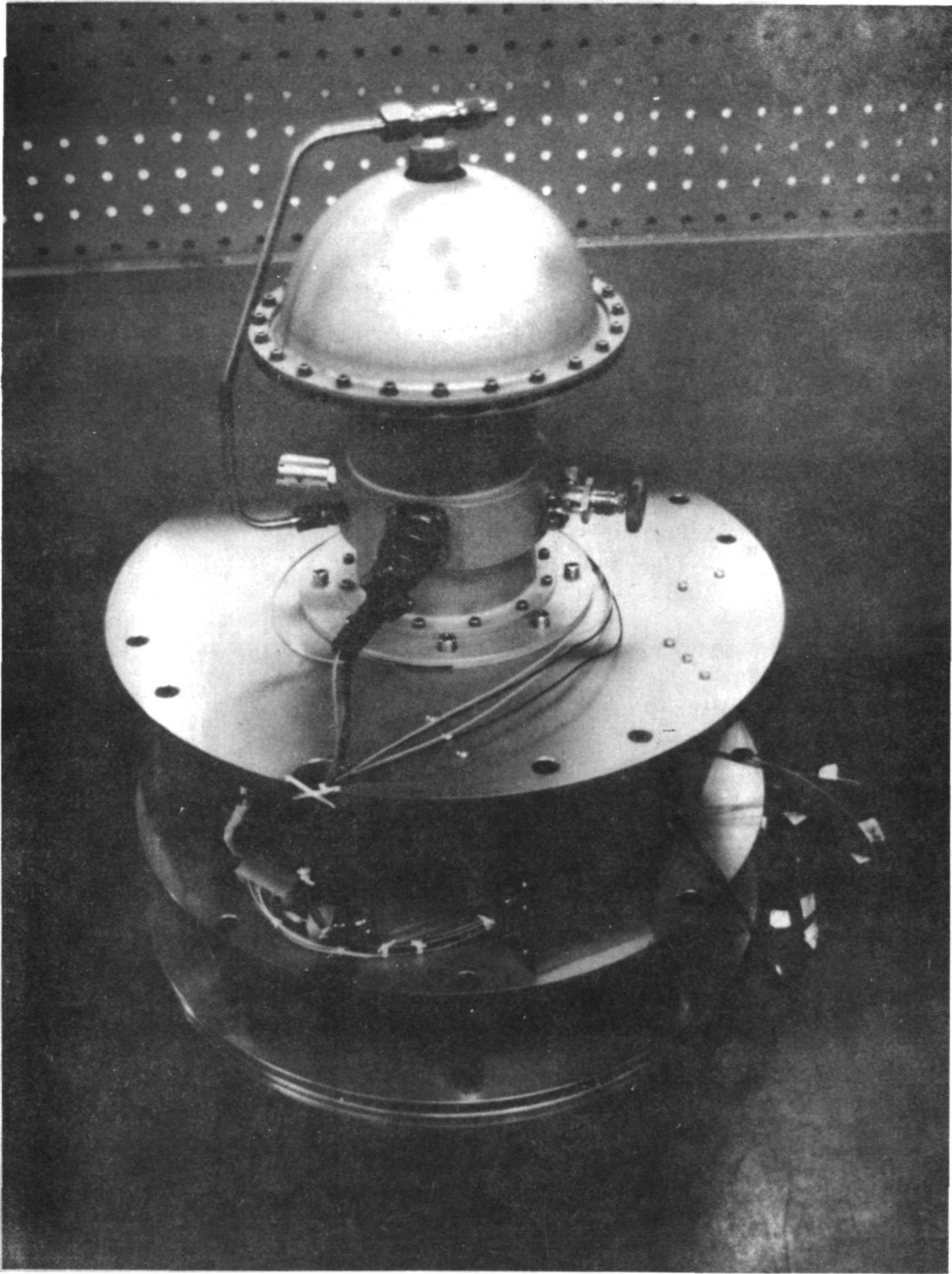


Figure 10. Unit mounted in a section of Black Brant VC Research Rocket NASA 21.006.

To eliminate the possibility of the Unit adversely affecting the rocket and/or other experiments on the rocket, a separate battery pack sized to operate the heater and solenoid valve is used. The battery pack used on NASA 21.006 is shown in Figure 10. It contains 24 Yardney HD-3 DC-2 Silvercels. The mass of this battery pack is 2.09 kg (4.6 lbm) and it is 0.188 m (7.4 in.) long by 0.087 m (3.44 in.) wide by 0.072 m (2.85 in.) high.

Each rocket is equipped with dual Haydon timers to provide a redundant means of sequencing both the rocket and payload events. These timers were used to close and open relays which started and stopped the flow of current to both the unit heater and solenoid valve.

Test Setup. Figure 11 shows the test setup used to obtain the time-temperature curves. A wooden cradle was made to support the Unit in such a way that the long axis of the capsule is in the horizontal plane and the air tube is on the top; this prevents the air tube from being filled with water before the heater housing is filled. The power supply in the foreground provided power for both the heater and solenoid valve. The combination switch and circuit breakers in the wire harness connecting the power supply to the unit were used to manually start and stop the heater and to open and close the solenoid valve during tests.

A time-temperature curve was made for each test. At first, a thermocouple was attached to the top of the capsule. However, this proved unsatisfactory because it did not indicate what was needed, the temperature at the center of the capsule where melting occurred last, and it indicated a much faster drop in temperature during water quench than actually occurred. To remedy this, a hole was drilled in the large end of the test capsule and the thermocouple was inserted to such a depth that it was in the center of the capsule. This produced satisfactory time-temperature curves and gave an indication of the relationship between the internally and externally mounted thermocouples.

Time-Temperature Tests. The purpose of these tests was to develop heating and cooling cycles which permit both phase changes of the capsule constituents — solid to liquid and liquid to solid — during the time it was in near-zero-g, above 91.44 km (56.82 mi).

The time above 91.44 km was 220 sec for NASA 13.113 (Fig. 2) as compared to 347 sec for NASA 21.006. Figures 12 and 13 show the time-temperature relationships developed for NASA 13.113 and NASA 21.006, respectively.

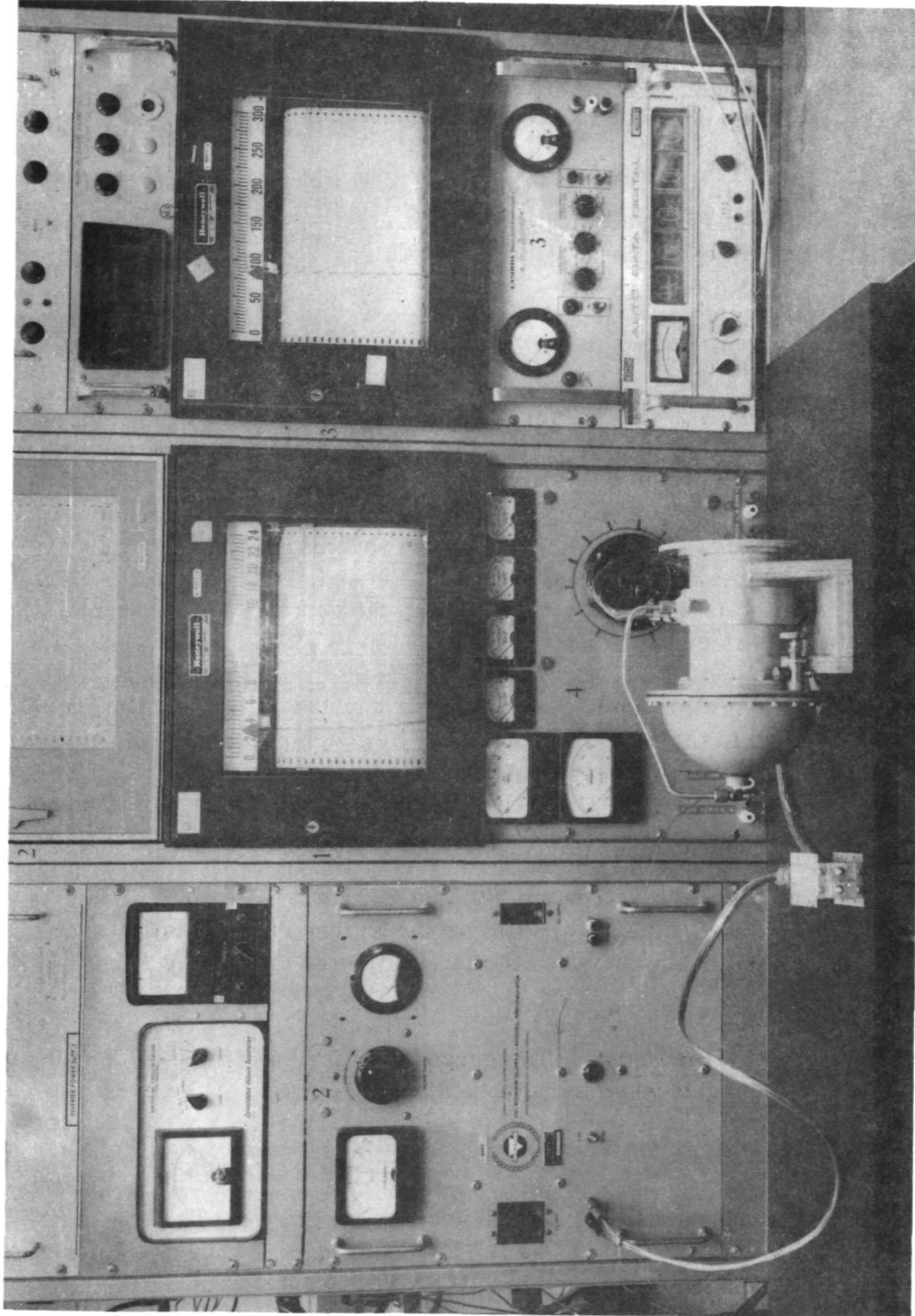


Figure 11. Test setup used to obtain time-temperature curves with capsule containing InBi and a thermocouple located at its center in the Unit.

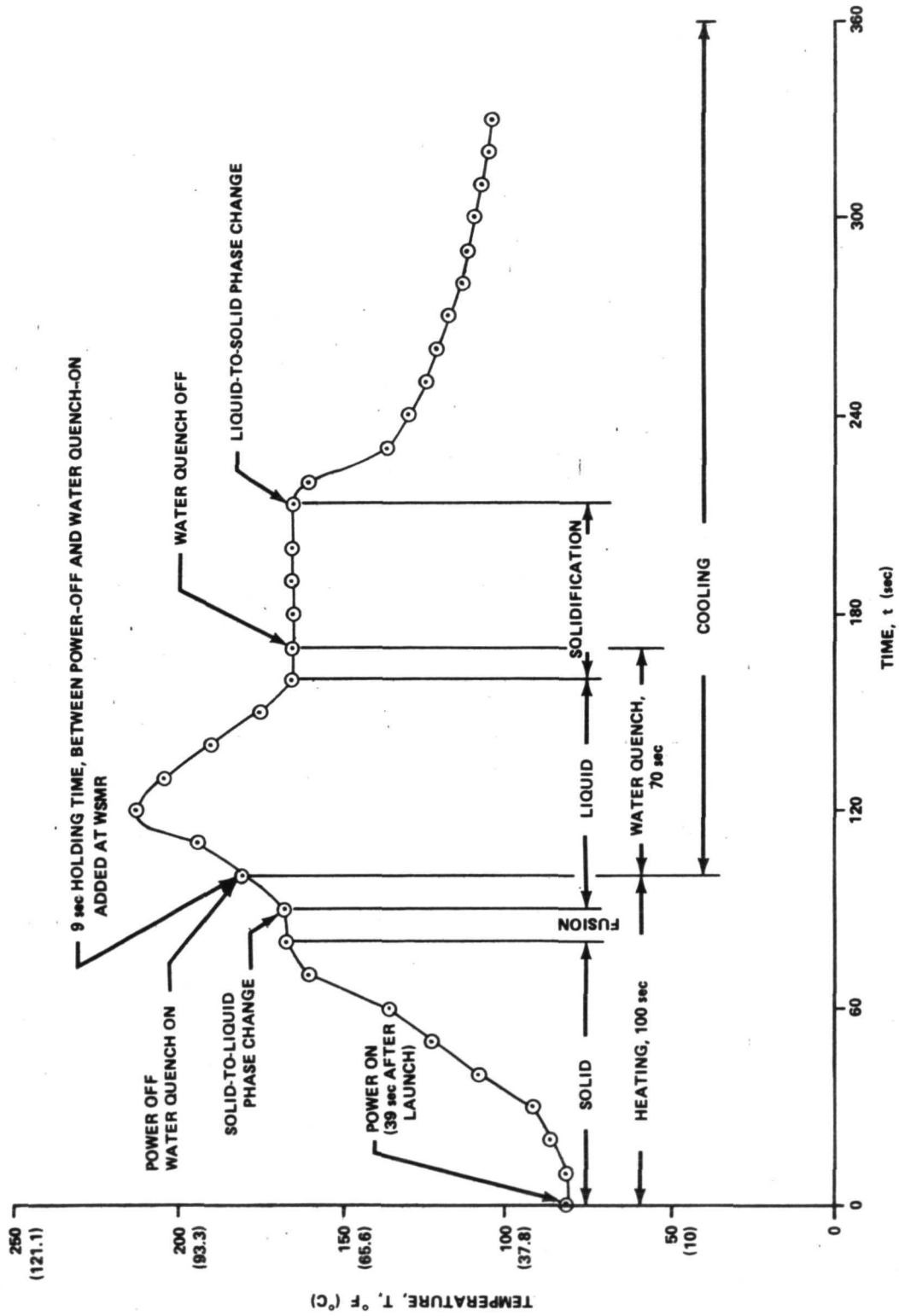


Figure 12. Time versus temperature relationship developed by MSFC for processing capsule on Aerobee 170A NASA 13.113.

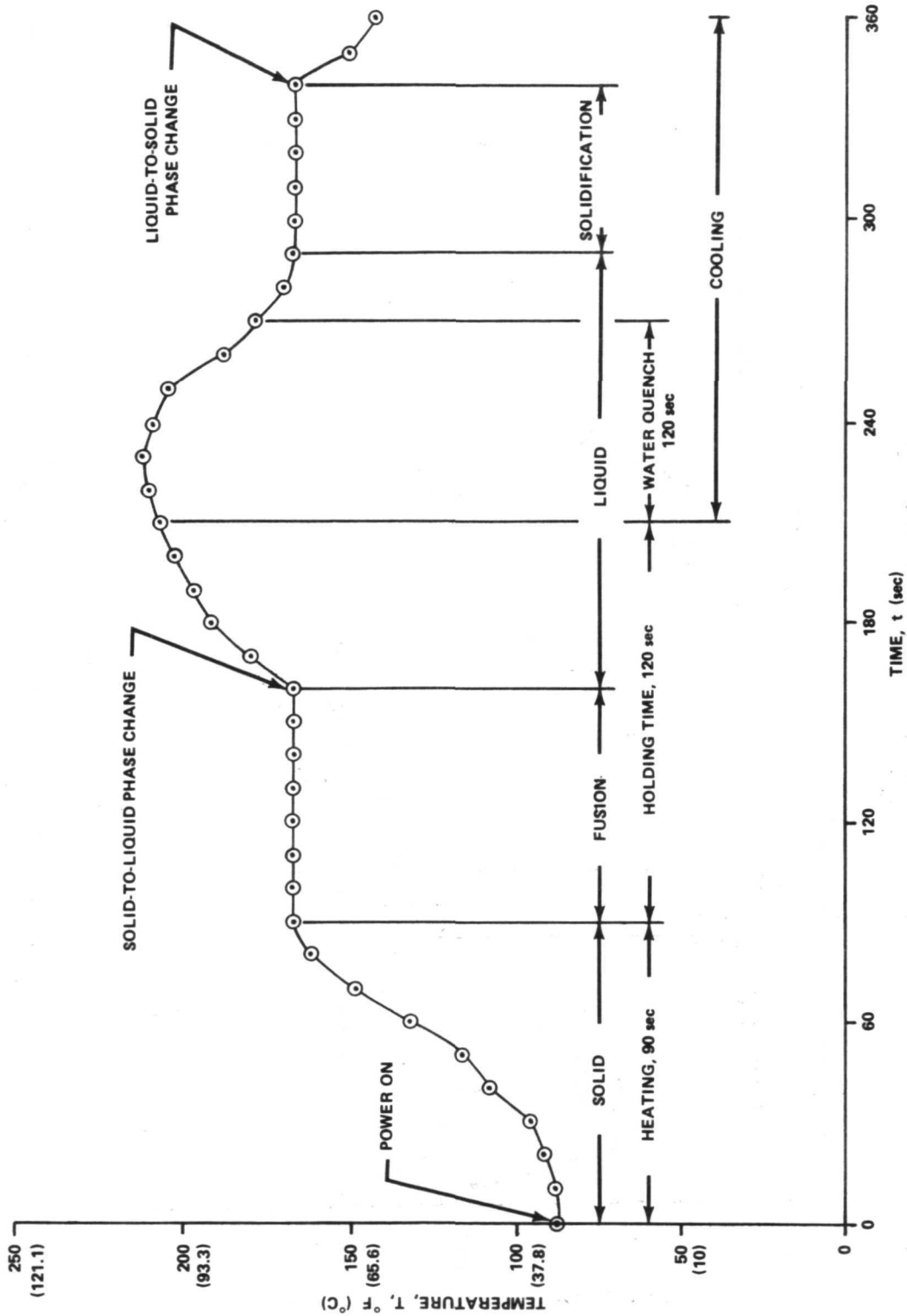


Figure 13. Time versus temperature relationship developed by MSFC for processing capsule on Black Brant VC NASA 21.006.

To accomplish both phase changes as described above for the NASA 13.113, it was necessary to keep to a minimum the time to change from solid to liquid and hold time in the liquid state. Several tests with various length heating times were conducted before 100 sec of heating for the NASA 13.113 and 90 sec for the NASA 21.006 were established. By increasing the heating time 10 sec, the time required for the solid-to-liquid phase change was reduced 60 sec, from 77 sec to 17 sec.

## Flight Data

### AEROBEE 170A RESEARCH ROCKET AND THE FLIGHT OF NASA 13.113

In Figure 14, the relationships between altitude versus time for Aerobee 170A NASA 13.113 and temperature versus time for the Temperature Control Unit are shown.

MSFC did not request any holding time because early tests indicated the specimen could not be cooled rapidly enough to obtain the liquid-to-solid phase change above 91.44 km (56.82 mi). However, by the time of the launch, October 19, 1971, MSFC had worked out a procedure where approximately 70 sec of holding time would have been the maximum. At White Sands Missile Range, Mr. Wuenscher requested that the timers be changed to provide 30 sec of holding time. GSFC was able to adjust the timers to provide 9 sec of holding time (Fig. 14).

After yo-yo despin, from 167.1 to 13.5 rpm, there is an acceleration of approximately 0.0018 g at the inner wall of the capsule as shown below.

### Acceleration at Inner Wall of Capsule Produced by Spinning (Fig. 15).

$$a_s = r \omega^2$$

where

$a_s$  acceleration produced by spinning at the inner wall of the capsule, in m/sec<sup>2</sup> (ft/sec<sup>2</sup>)

$r$  radius of the capsule, in m (in.)

$\omega$  angular velocity of the vehicle after despin, in radians/sec

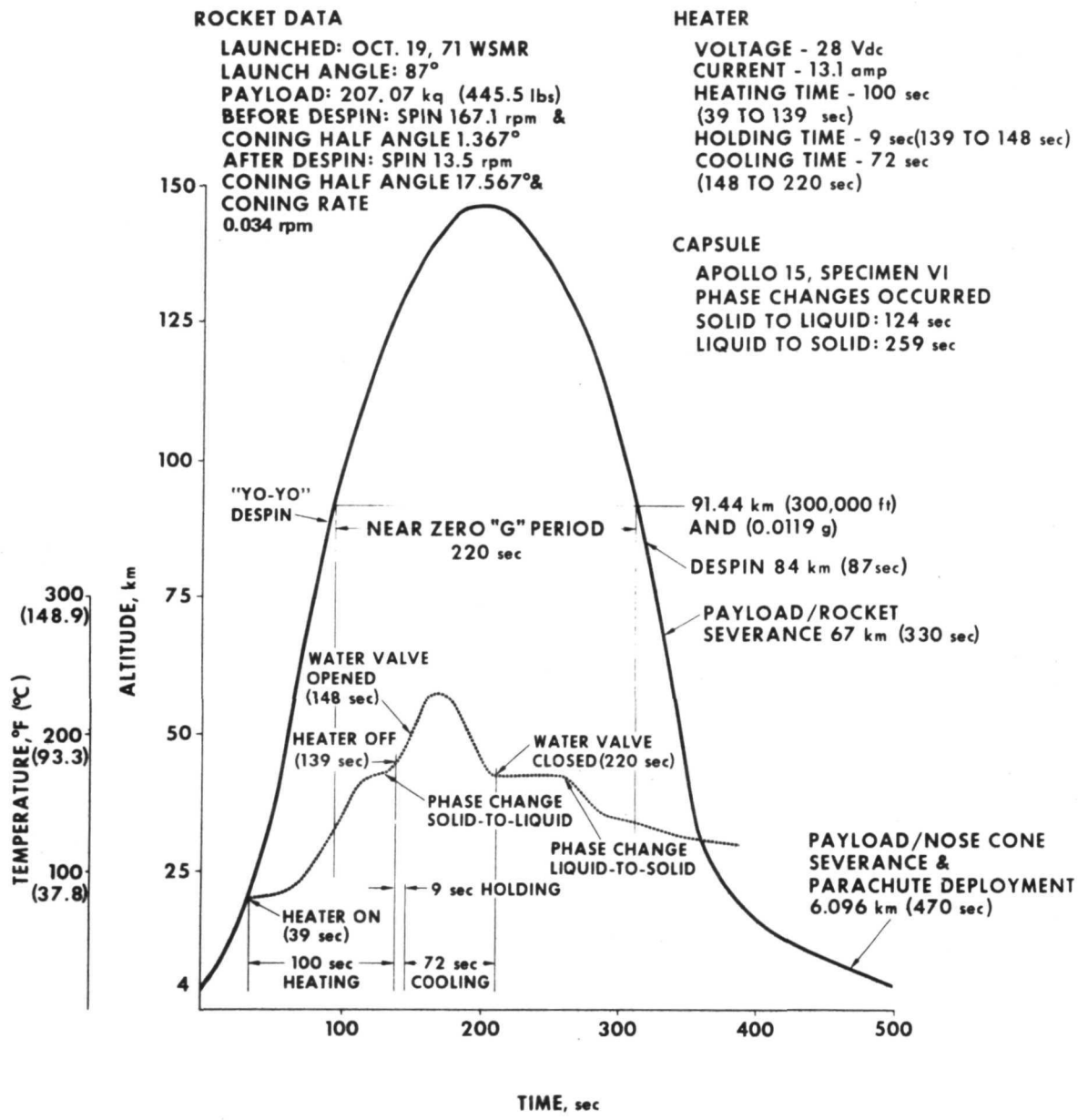


Figure 14. Altitude versus time for Aerobee 170A NASA 13.113 and temperature versus time for Temperature Control Unit.

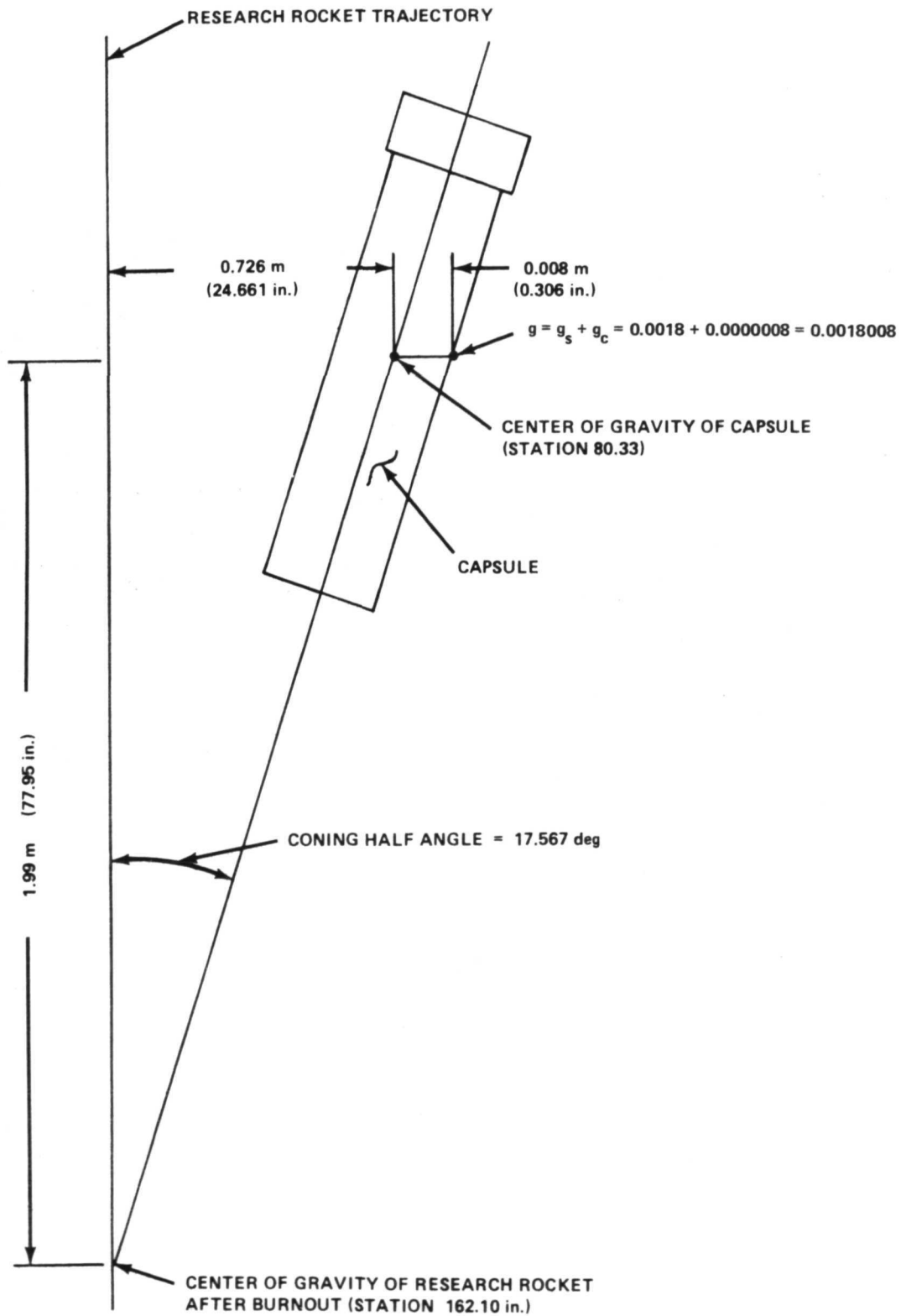


Figure 15. Acceleration at inner wall of capsule produced by spinning and coning of Aerobee 170A NASA 13.113.



$$a_s = \frac{0.690 \text{ in.}}{2} \times \frac{1 \text{ ft}}{12 \text{ in.}} \times (1.417 \text{ rad/sec})^2$$

$$a_s = 0.058 \text{ ft/sec}^2$$

$$g_s = \frac{a_s}{32.16 \text{ ft/sec}^2} = \frac{0.058}{32.16} = 0.0018 \text{ g}$$

Acceleration at Inner Wall of Capsule Produced by Coning (Fig. 15).

$$a_c = r \omega'^2$$

where

$a_c$  acceleration produced by coning at the inner wall of the capsule, in in./sec<sup>2</sup> (ft/sec<sup>2</sup>)

$r$  distance from research rocket trajectory to inner wall of capsule

$\omega'$  coning rate, in radians/sec

$$a_c = \left( 81.77 \text{ in.} \times \sin 17.567 \text{ deg} + \frac{0.690 \text{ in.}}{2} \right. \\ \left. \div \cos 17.567 \text{ deg} \right) \frac{1 \text{ ft}}{12 \text{ in.}} \times (0.00357 \text{ rad/sec})^2$$

$$a_c = \frac{24.661 + 0.362}{12} \times 0.0000128$$

$$a_c = 0.000025 \text{ ft/sec}^2$$

$$g_c = \frac{a_c}{32.16 \text{ ft/sec}^2} = 0.0000008 \text{ g}$$

$$g = g_s + g_c$$

$$g = 0.0018 + 0.0000008 = 0.0018008$$

# Capsule

## OBJECTIVE

The objective of the experiment was to investigate the stability of gas bubbles in plain and fiber-reinforced metal melted and solidified in a near-zero-g environment.

## DESCRIPTION OF SAMPLE

The sample originally designed and fabricated for the Apollo 15 Composite Casting Demonstration by General Dynamics/Convair was made up of two material systems: interconnected gas cells in a fiber-reinforced metal matrix in the A-half of the sample and discrete gas bubbles in plain metal matrix in the B-half of the sample. The A-half was made up of 11 disks of InBi-coated copper wire layups which formed interconnected gas cells. The B-half was made up of 20 disks of InBi eutectic alloy which had been coined to form 27 half-spherical impressions in each side. When the disks were stacked, discrete uniformly distributed spheres were formed. The two halves, separated by an aluminum divider, were placed into an aluminum sample capsule as shown in Figure 16 and were capped in an argon chamber. The sample capsule was, subsequently, sealed by electron beam welding.

## PREPARATION AND PROCESSING OF SAMPLE

A-Half, Interconnected Gas Cells. Lengths of 0.0001 m (0.005 in.) beryllium copper wire were coated with the InBi eutectic alloy by placing four wires into a 0.001 m (0.045 in.) I.D. plastic tube and injecting molten InBi into the tube while it was immersed in a hot water bath as shown in Figure 17. After the tube was filled, it was removed from the hot water bath and straightened. The InBi solidified in a few minutes after removal from the bath. The plastic tubing was then stripped from the InBi-coated copper wires. The coated wires were straightened, cut to length, and layed up in a tool as shown in Figure 18. The layup was compressed in a platen press as shown in Figure 19 to a finished thickness of approximately 0.003 m (0.140 in.). Disks 0.017 m (0.687 in.) in diameter were then cut from the layup as shown in Figure 20. An enlarged view of the cells formed by the coated wires is shown in Figure 21. The sample half was then assembled in a chamber filled with argon by stacking 11 disks in an assembly fixture and compressing them to the final dimension of 0.037 m (1.440 in.).

B-Half, Discrete Gas Bubbles. Cast rods of InBi eutectic alloy were cut into slices which were then coined using tooling shown in Figure 22 and

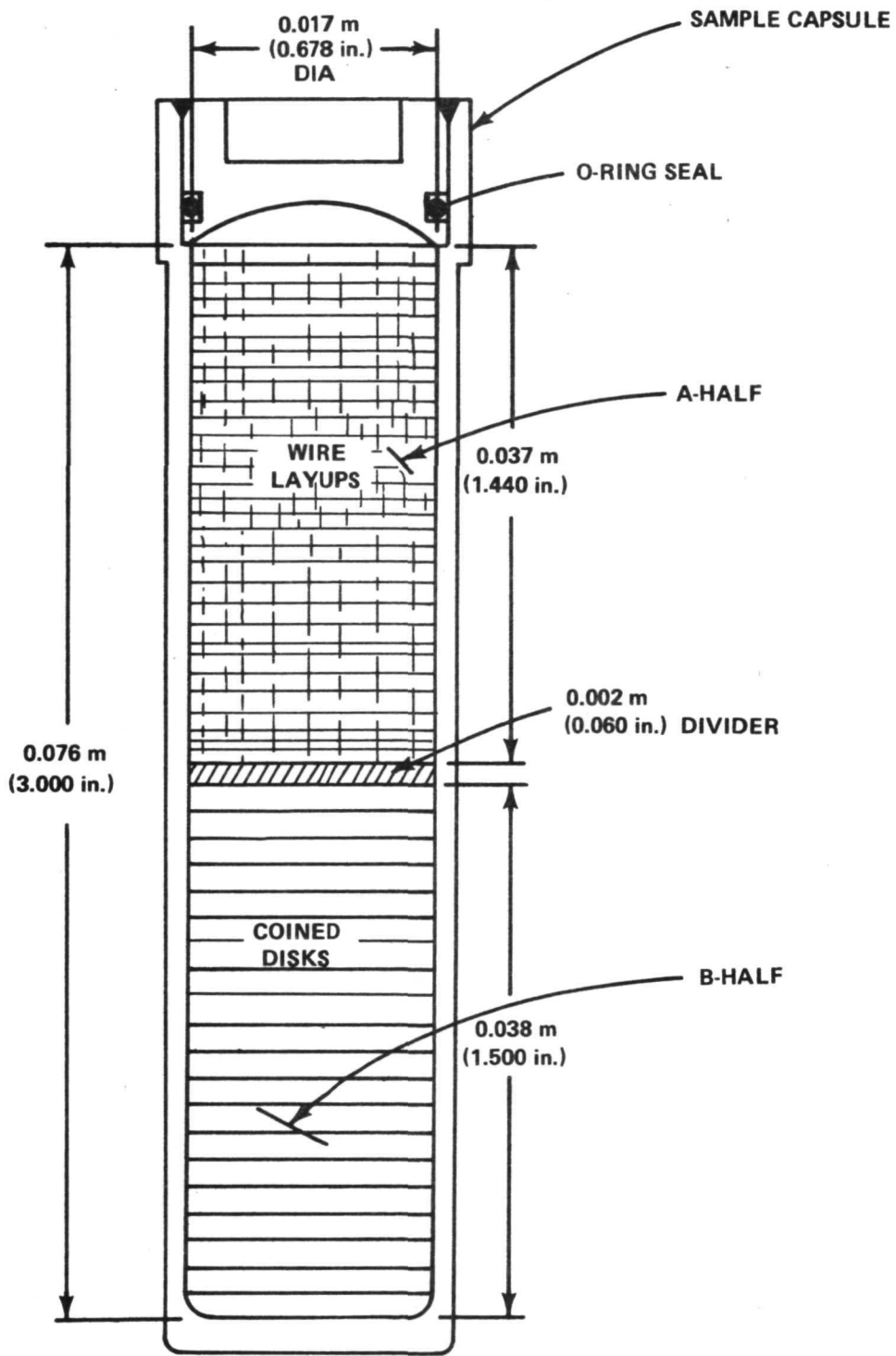


Figure 16. Sample configuration.

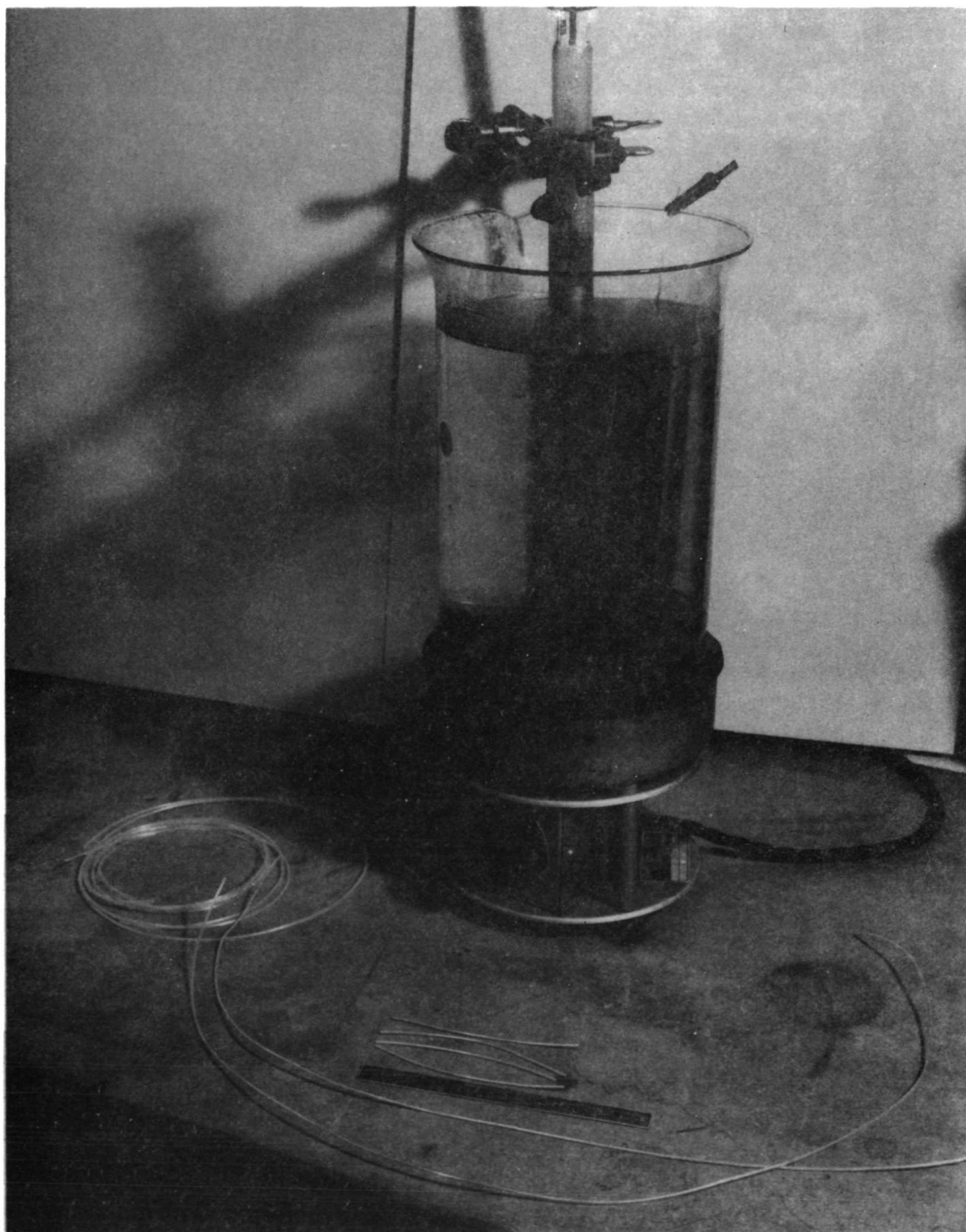


Figure 17. Casting of layup wires — molten InBi injected in 0.76 m (30 in.) long plastic tube 0.001 m (0.045 in.) in diameter containing 4 Cu-Be wires 0.001 m (0.005 in.) in diameter.

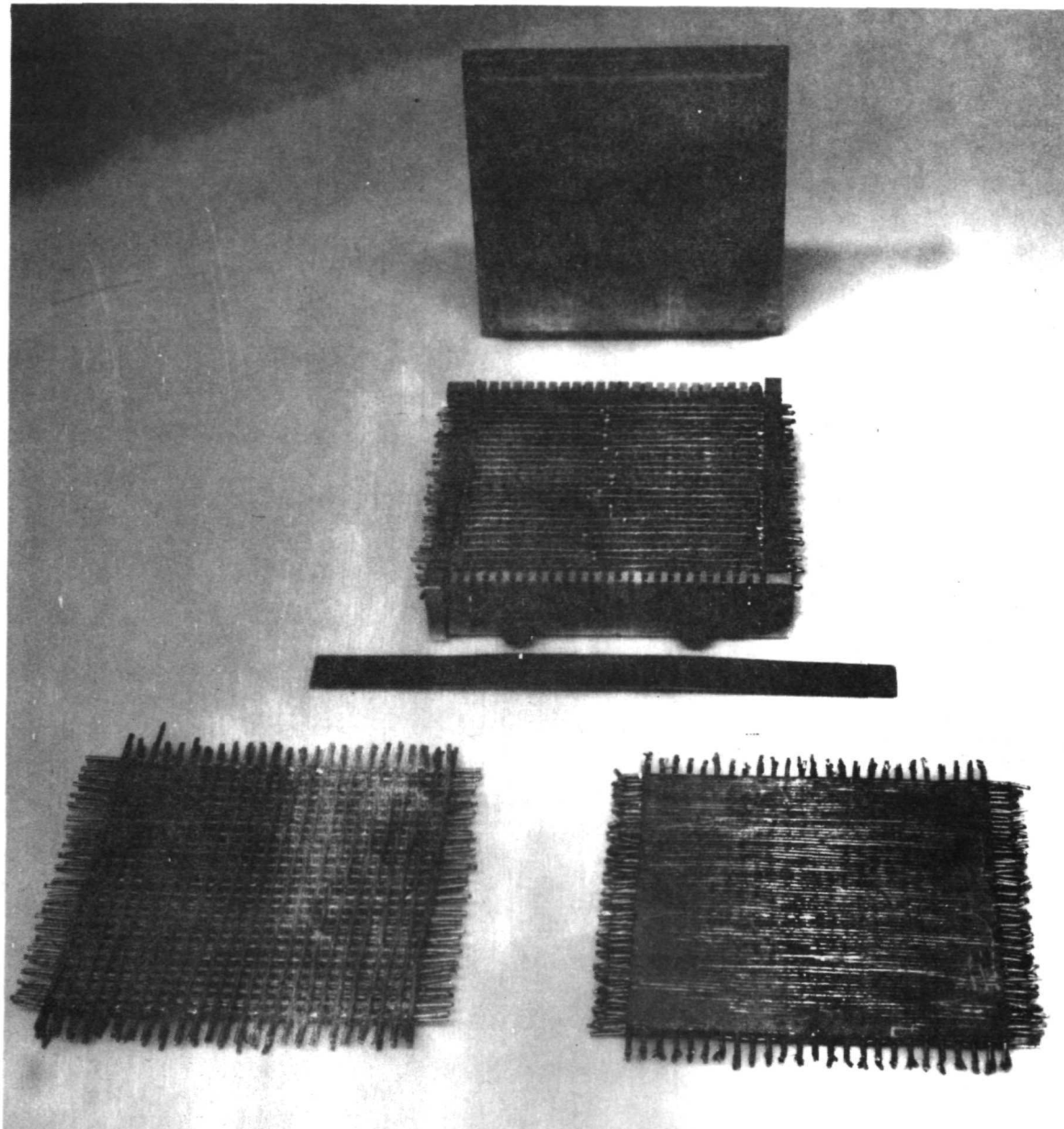


Figure 18. Layup at various stages of assembly and layup tooling.

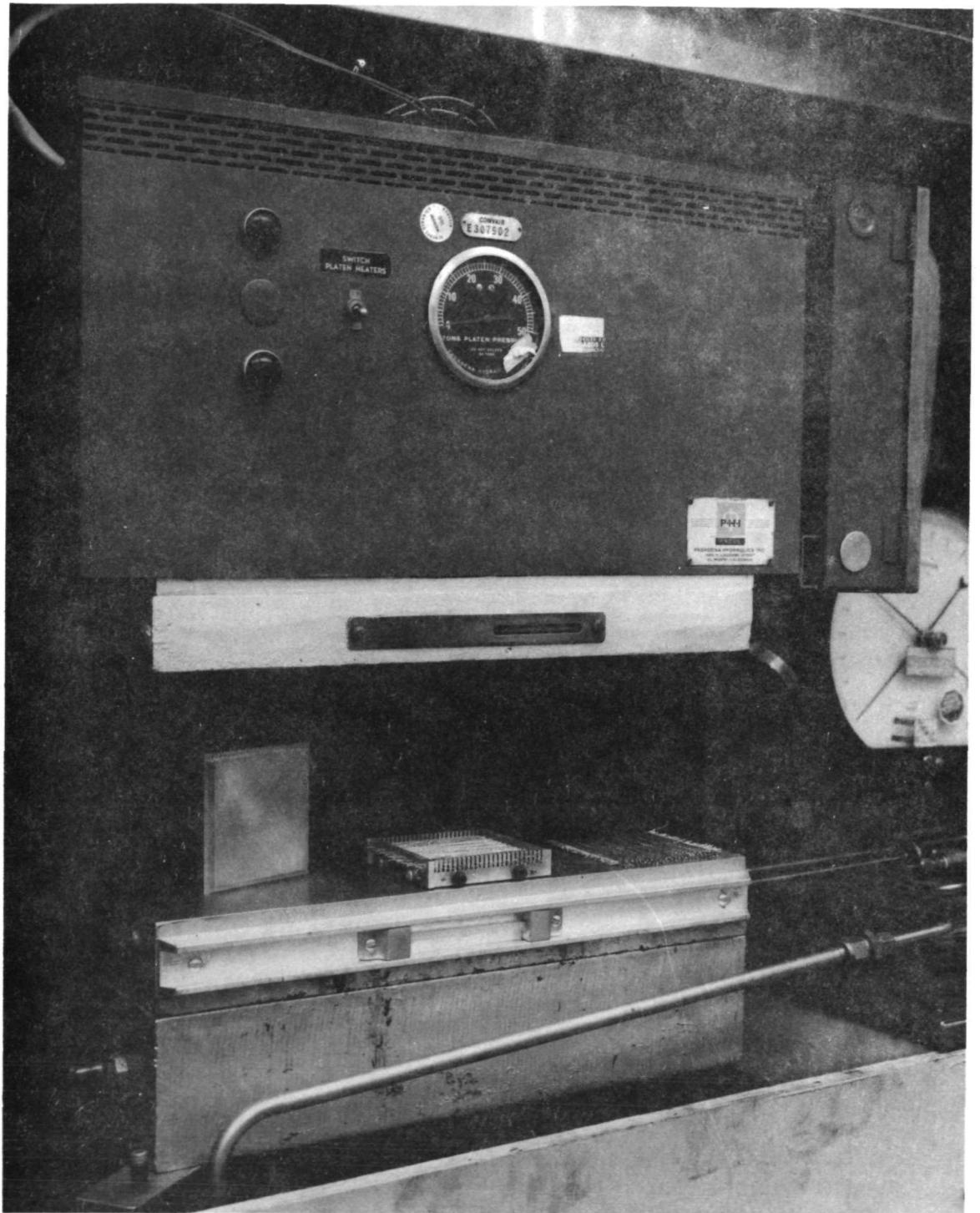


Figure 19. Layup in press for bonding.

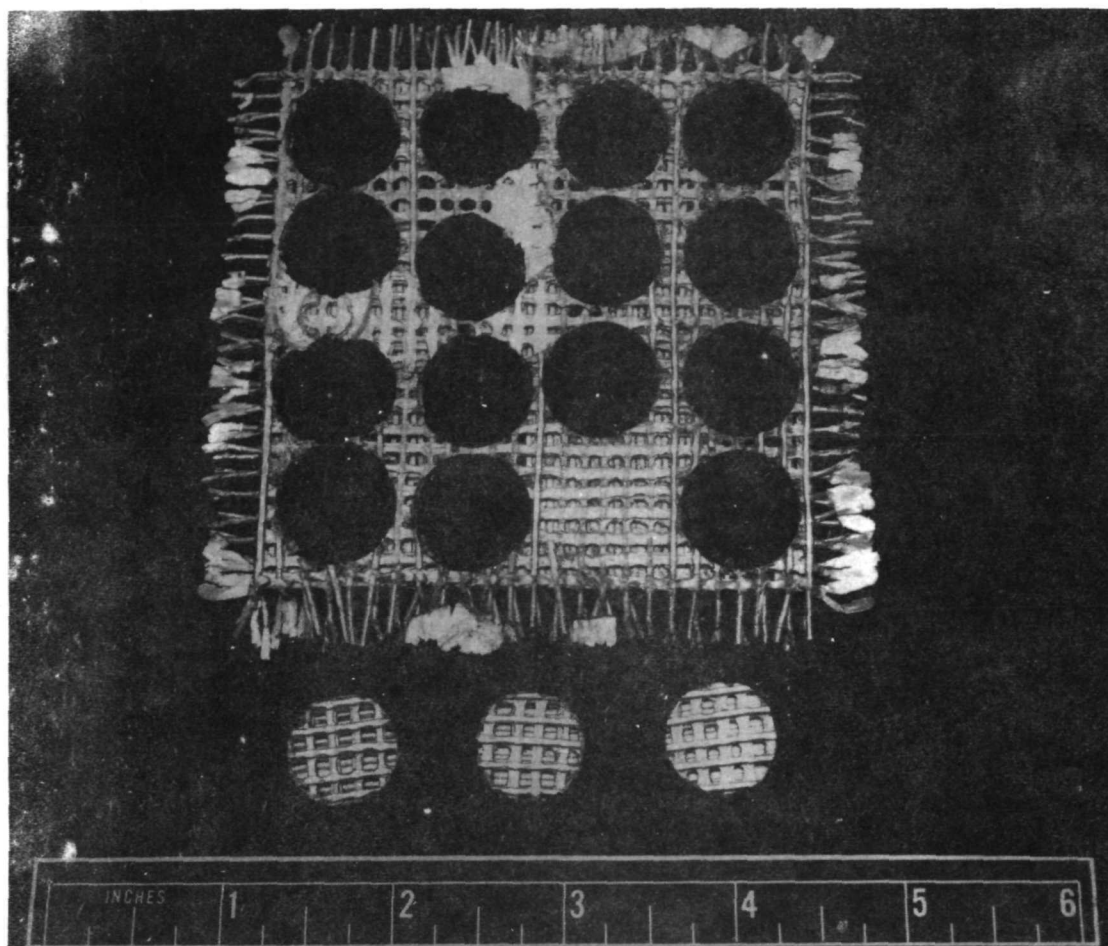


Figure 20. Cutting of layup disks — first layup  
(subsequent disks were more perfect).

the press shown in Figure 23. A finished coin is shown in Figure 24. The coins were cleaned and stacks of 20 disks were bonded together by compressing them at 60° C (140° F) to the finished length of 0.038 m (1.5 in.) in a chamber filled with argon (Fig. 25). The bonded stack was removed from the tool and turned to 0.017 m (0.687 in.) O.D. A section cut from an assembled sample is shown in Figure 26.

Sample Assembly. The A and B sample halves were inserted into an aluminum sample capsule and capped in a chamber filled with argon. Final sealing of the capsule was accomplished by electron beam welding the cap to the capsule.

Processing of Sample. The flight sample was processed in the Unit as shown in Figures 25, 26, 27 and 28.



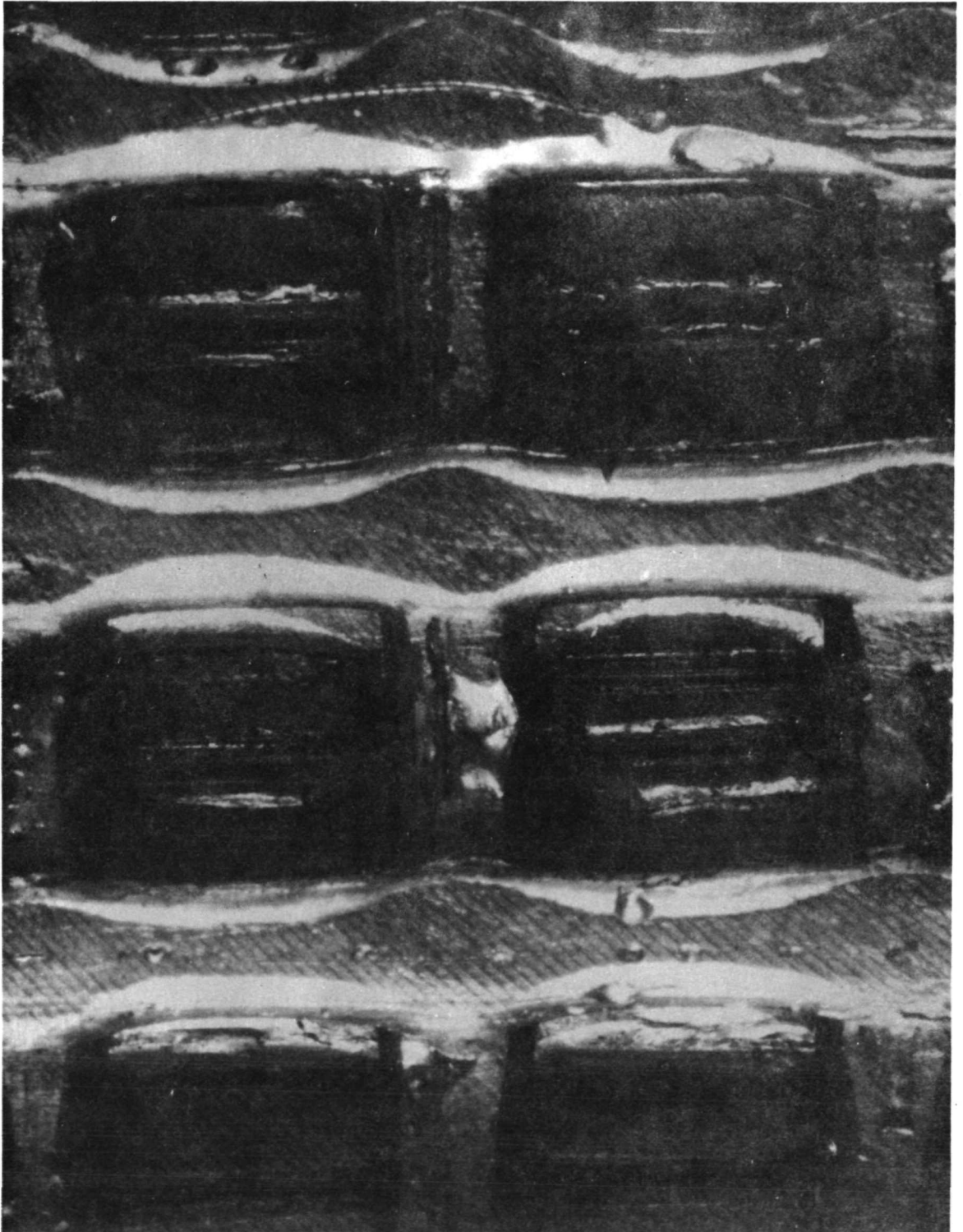


Figure 21. Layup cells (approximately 25X) [cell spacing between wired center lines approximately 0.003 m (0.130 in.)].



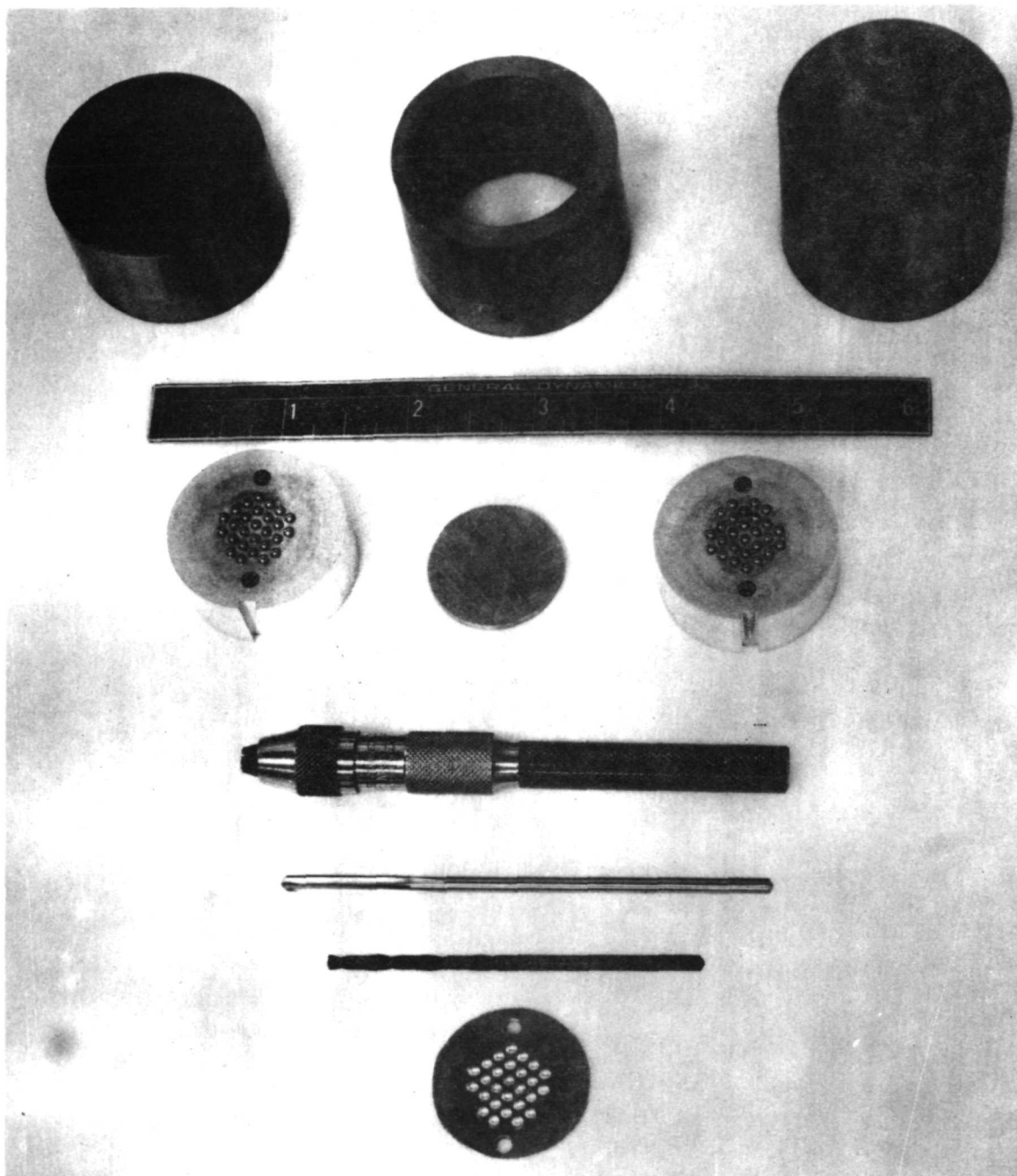


Figure 22. Coin tooling.

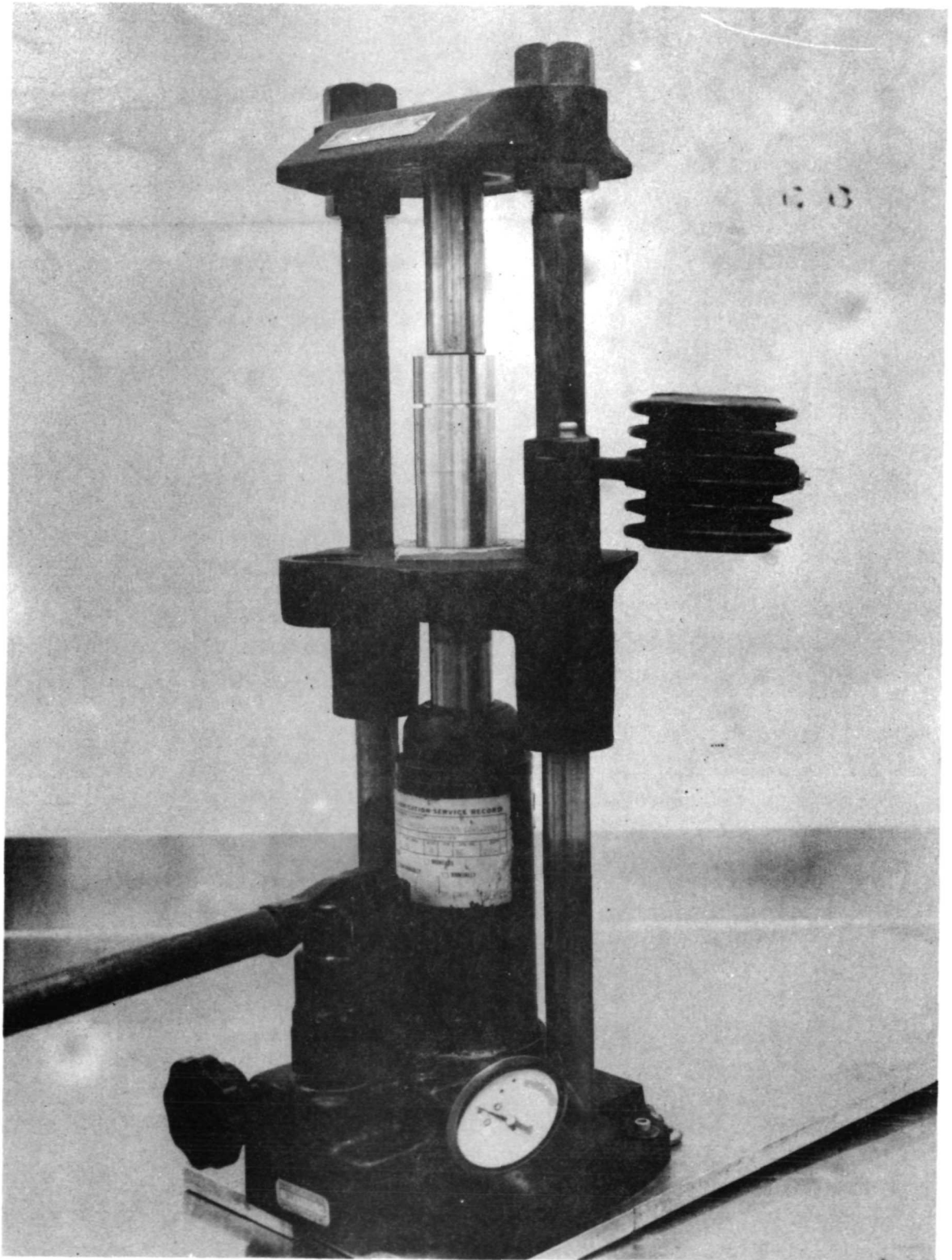


Figure 23. Tooling for coins in press (used for manufacture of coins and for bonding of stack).

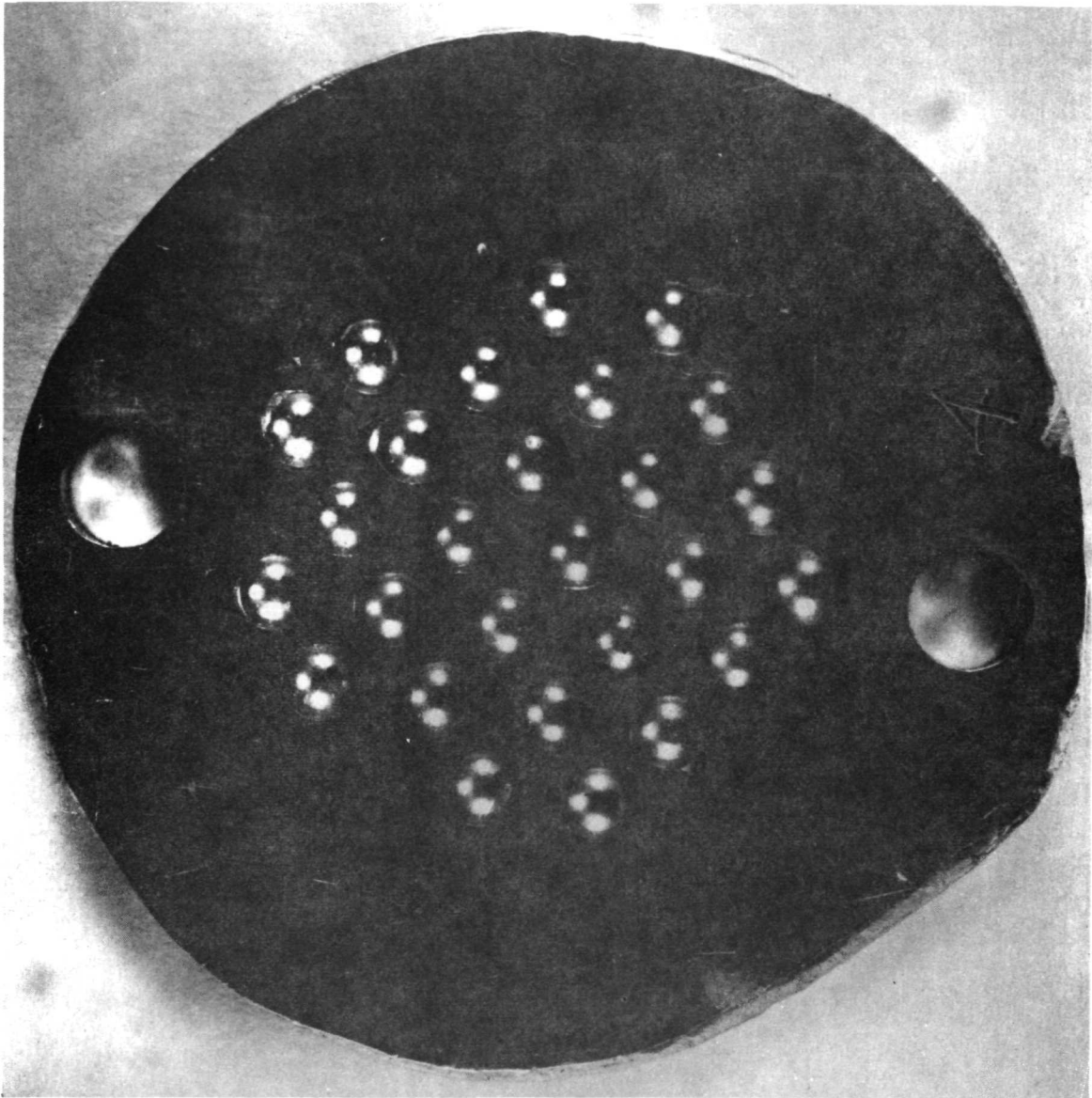


Figure 24. Finished coin (plain InBi).

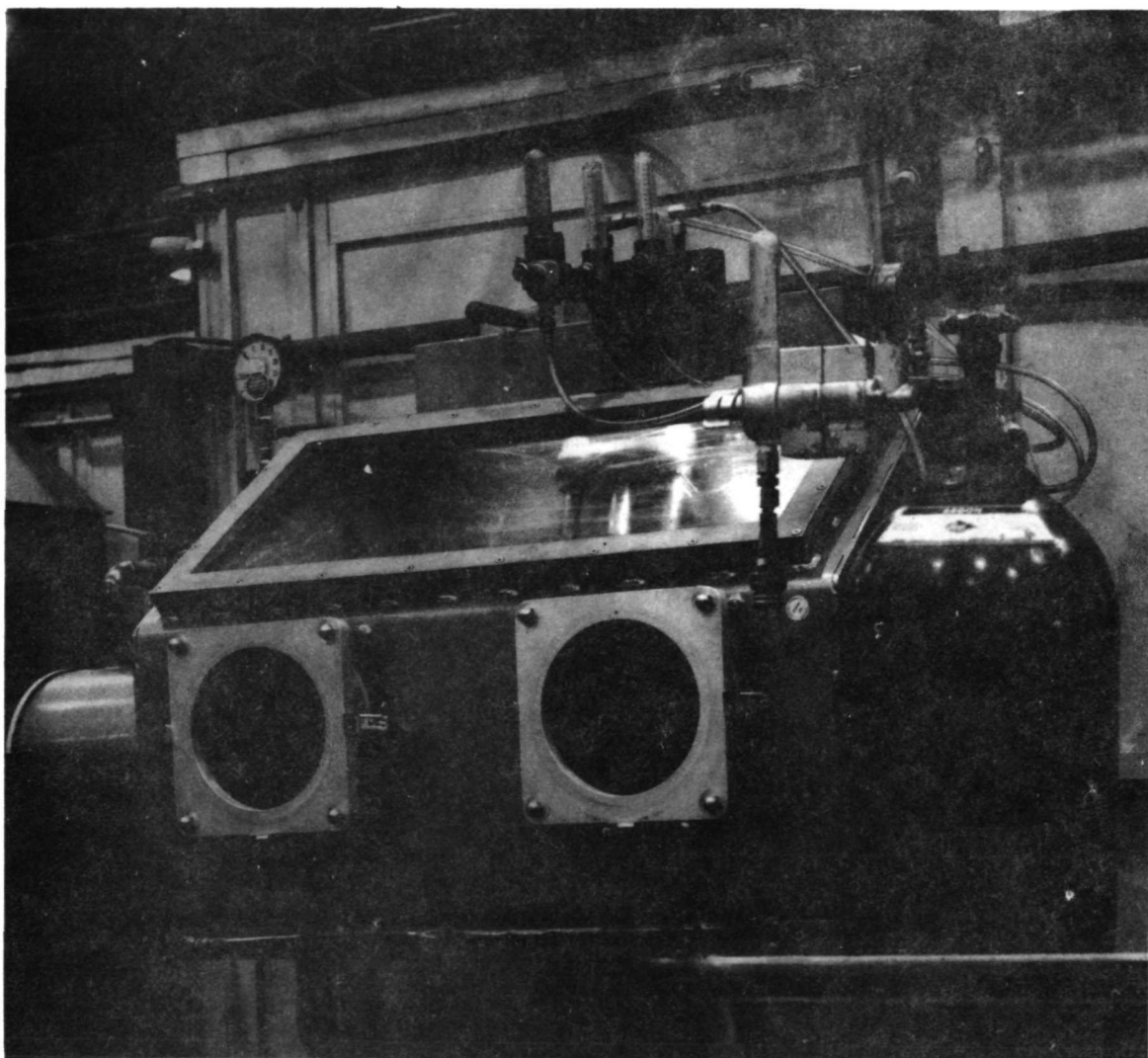


Figure 25. Argon filled chamber used for sample assembly.

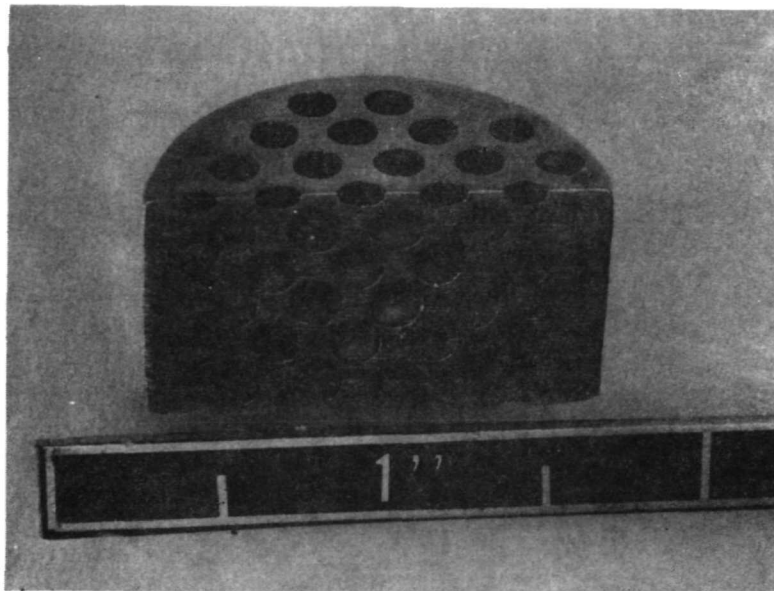


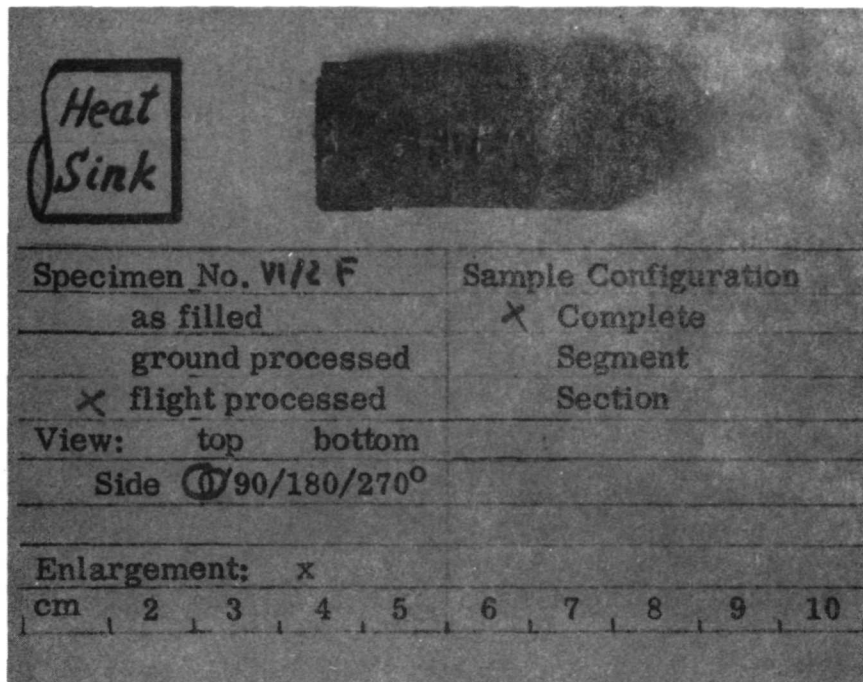
Figure 26. Section of B sample.

An identical ground control sample was processed in the same equipment using the same procedures. The sample was in the horizontal position; therefore, gravity forces were acting perpendicular to the long axis.

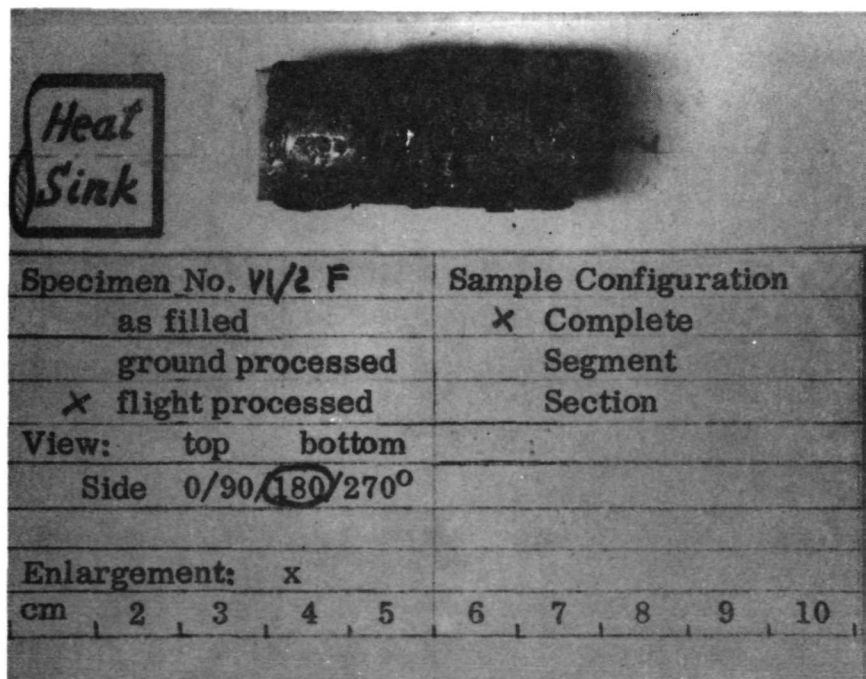
#### EVALUATION OF SAMPLE

Removal from Capsule and Preliminary Evaluation. Both the flight and ground control samples were sectioned longitudinally using the electrical discharge machining (EDM) technique. The samples were sectioned while in the aluminum capsule to simplify holding the sample. Unfortunately the flight sample had shrunk slightly and rotated during the cutting operation. Consequently, the finished cut was irregular and additional material was inadvertently removed from one end of the sample.

Examination of the flight sample revealed that the A-half of the sample had not been heated sufficiently to melt the InBi coating on the wires except in a small area as seen in Figure 27. Therefore, further evaluation of this sample half was not performed.



a



b

Figure 27. A sample half as removed from capsule.



The B-half of the sample had melted considerably more as evidenced by the appearance of the external surfaces as seen in Figure 28 and the sectioned surfaces as seen in Figure 29. More melting obviously occurred in the end of the sample nearest the bottom of the capsule (heat sink) and in the half identified as VI/IF-B in Figures 28b and 29b. Some bubble coalescence did occur in this portion of the sample.

Detailed Evaluation of B-half of Sample. The sectioned sample halves, both flight and ground control, were mounted in plastic, polished, and etched for more detailed evaluation.

The ground control sample shown in Figures 30 and 31 appears to have melted throughout and most of the gas bubbles have been eliminated due to buoyancy forces.

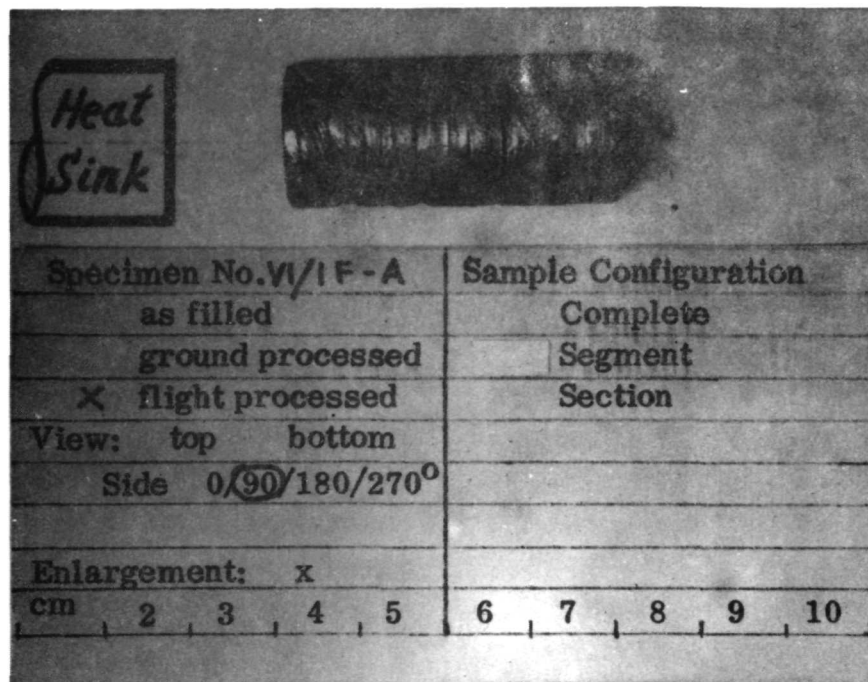
Longitudinal sections of the flight sample are shown in Figures 32 and 33 after initial preparation. These photomicrographs show that only partial melting occurred in the sample. In the areas which appeared to have melted, three conditions were noted: Some bubbles had disappeared, some bubbles had coalesced, and some bubbles remained in place.

At this point a decision was made to polish the sample sections further to expose other layers of bubbles. The section identified as VI/IF-A was remounted in plastic so that it could be polished in the transverse direction.

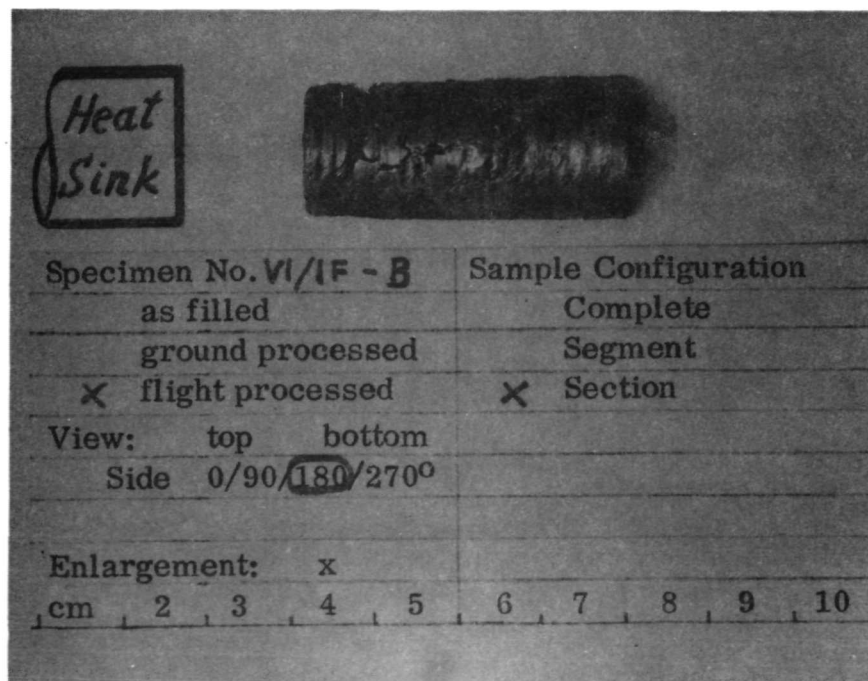
Further polishing and etching of the longitudinal section VI/IF-B shown in Figure 34 revealed two distinct zones. The lighter area with the variation in structure at the left and top of the photomicrograph is the melted zone. The darker area at the bottom right is the unmelted, or unaffected, zone. Photomicrographs of the circled areas in Figure 34 are shown in Figures 35, 36, 37, and 38. These show the microstructure in the melted zone, at the transition, and in the unmelted zone. The microstructure of the unmelted area (Fig. 38) is comparable to that taken from an as-coined disk (Figs. 39, 40, and 41).

Further polishing and etching of section VI/IF-A in the transverse direction showed similar structure (Fig. 42). Photomicrographs of the areas in melted, transition, and unmelted zones are shown in Figures 43, 44, and 45.

Additional cuts made through each section of the sample show similar structures. The wide variations in structure throughout the flight sample are indicative of its complex thermal history. Obviously, the sample did not approach an equilibrium temperature.



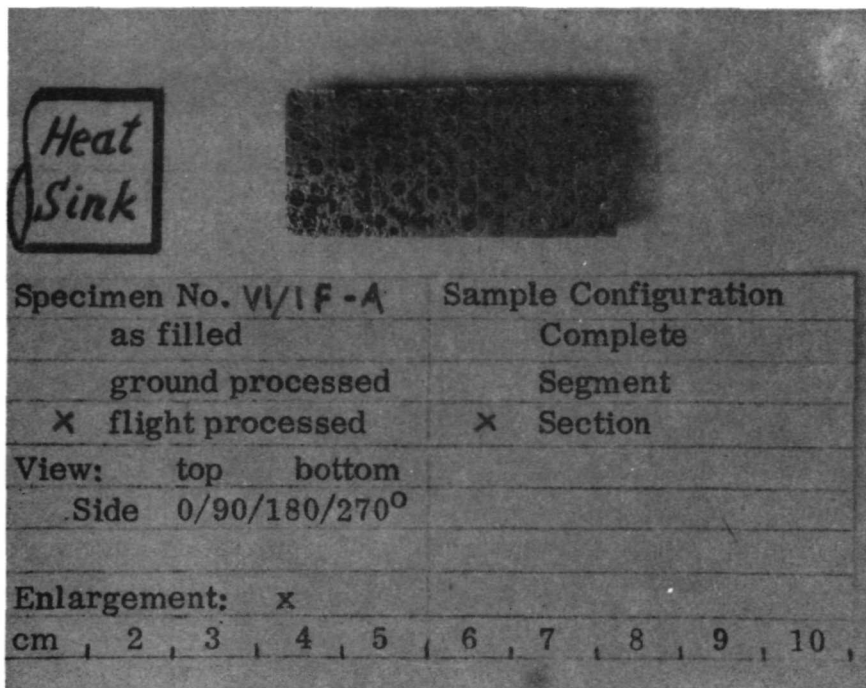
a



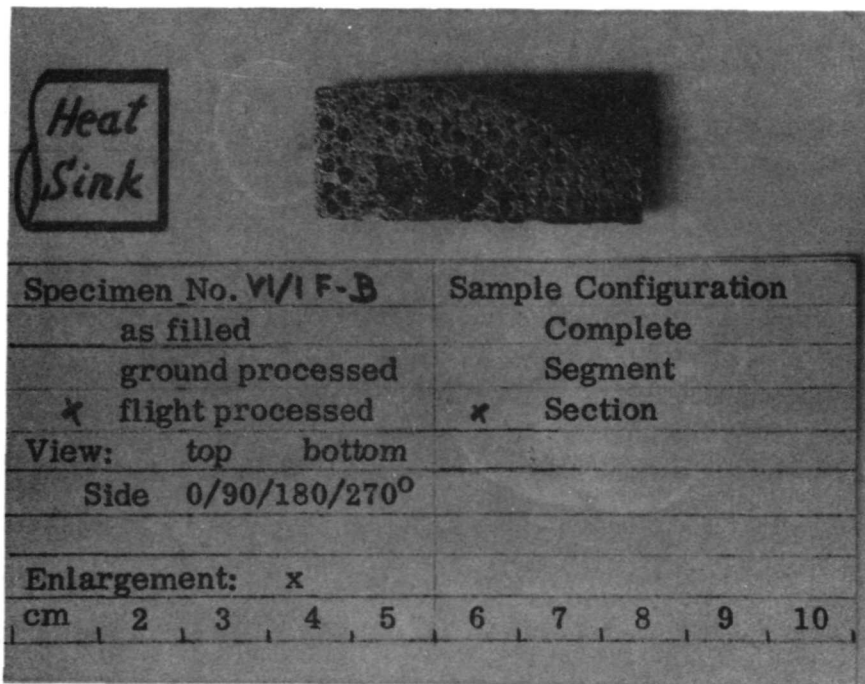
b

Figure 28. B sample half, external surface as removed from capsule.





a



b

Figure 29. B sample, longitudinal sections as sectioned.

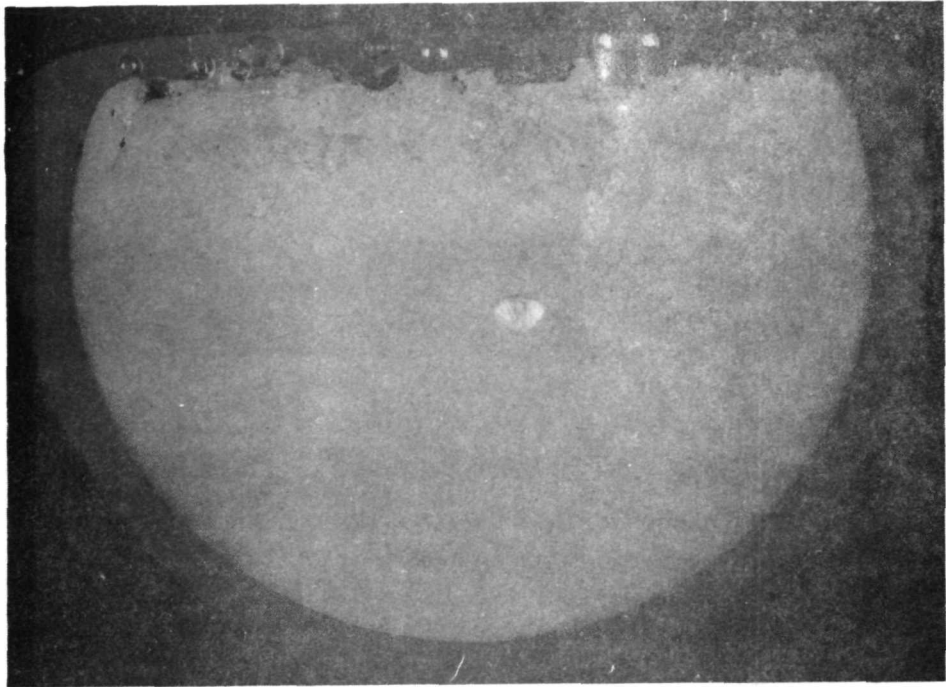


Figure 30. Transverse section of ground control sample (6X).

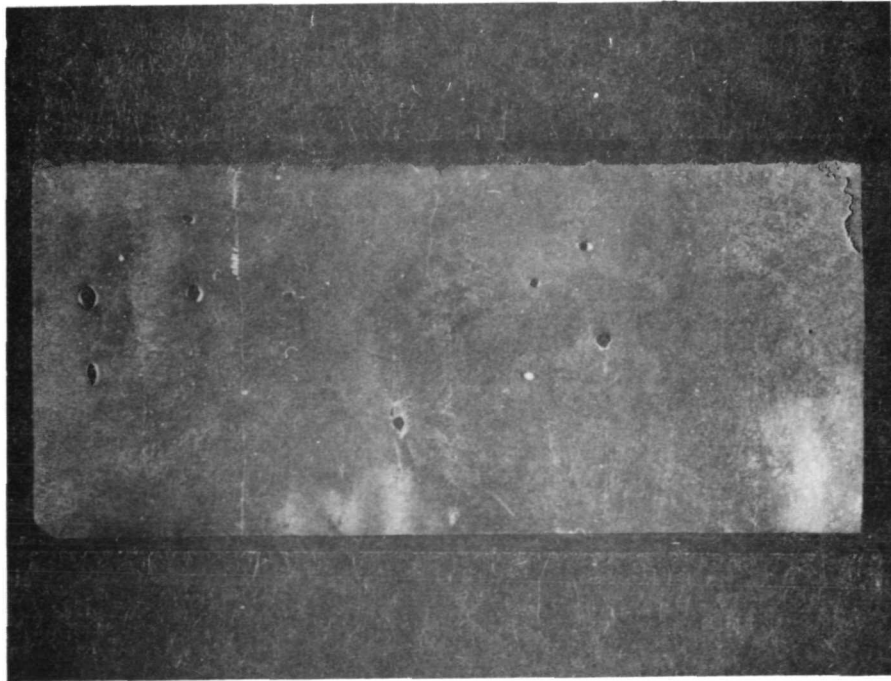


Figure 31. Longitudinal section of ground control sample (4X).

Bottom  
of  
Sample

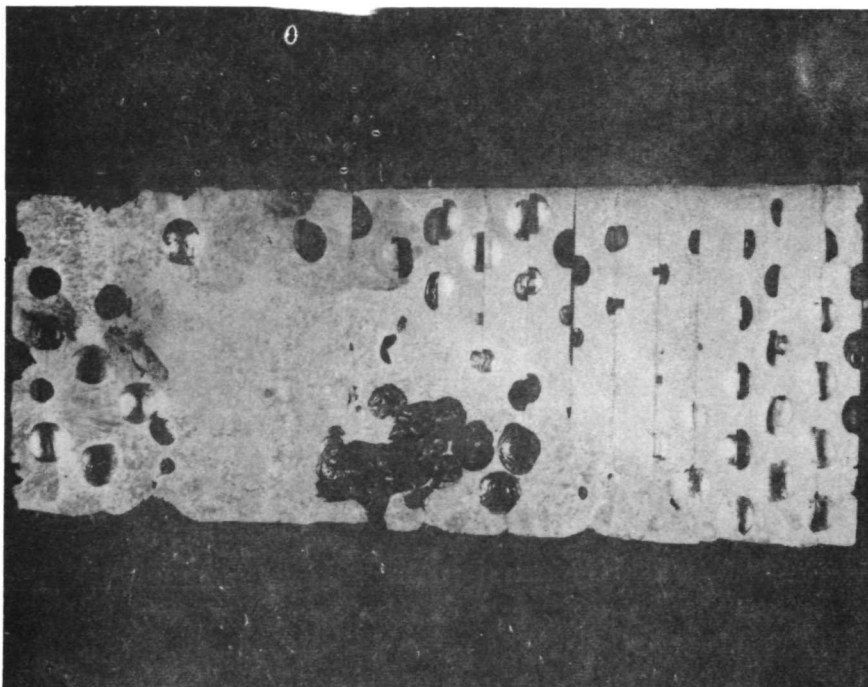


Figure 32. Longitudinal section of flight sample VI/IF-B (3X).

Bottom  
of  
Sample

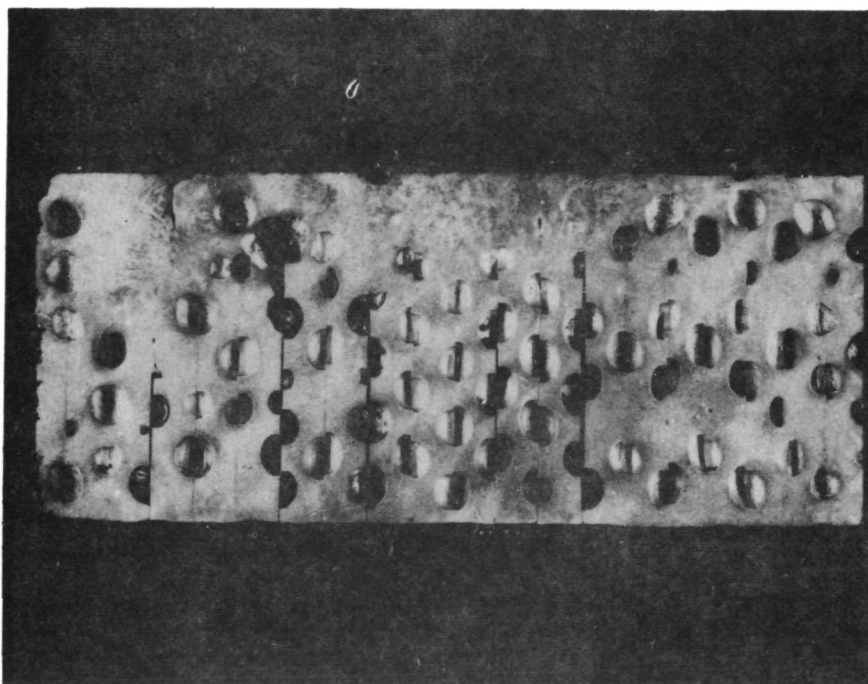


Figure 33. Longitudinal section of flight sample VI/IF-A (2.75X).

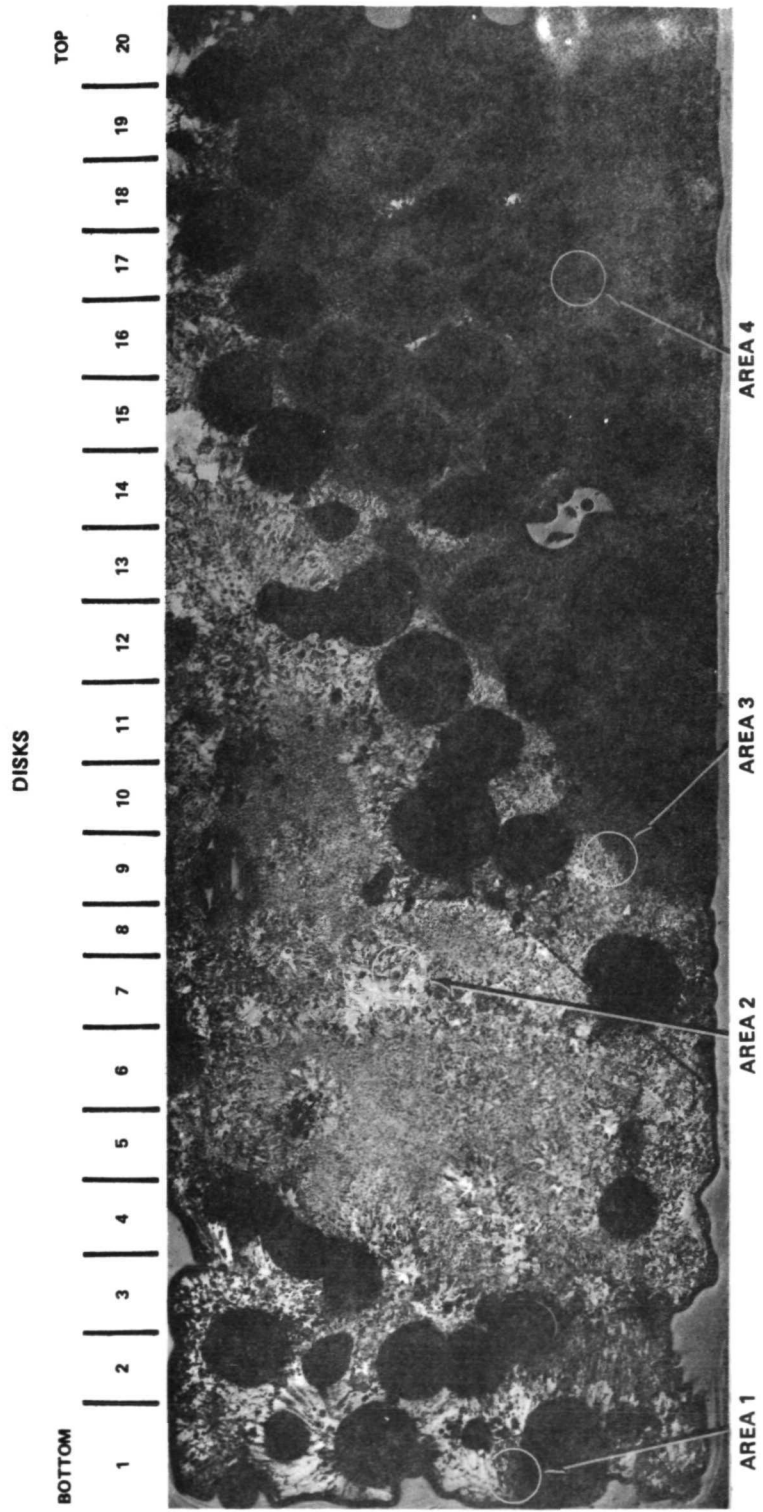


Figure 34. Longitudinal section VI/IF-B showing etched macrostructure of Aerobee wafer composite (Areas 1 through 4 were documented to show recrystallized structure resulting from flight test, transition zone, and unaffected structure) (7X).

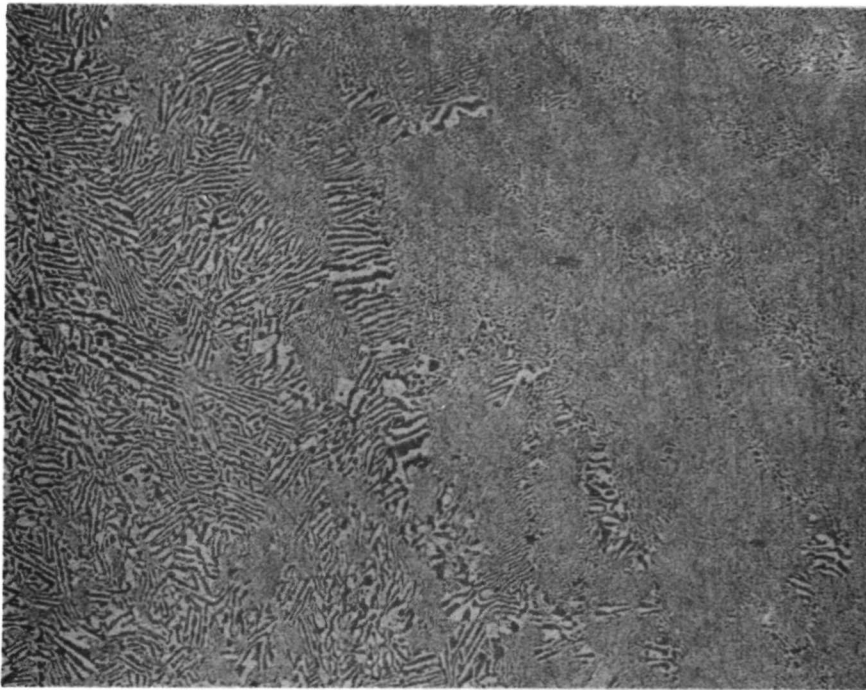


Figure 35. Microstructure at Area 1, Figure 34 (100X).

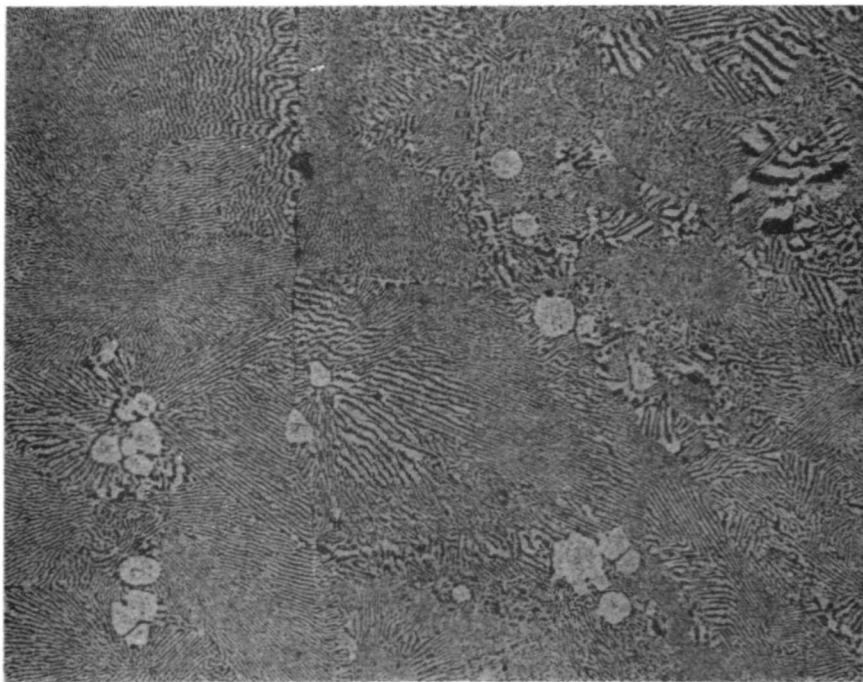


Figure 36. Microstructure in melted area at Area 2, Figure 34 (100X).

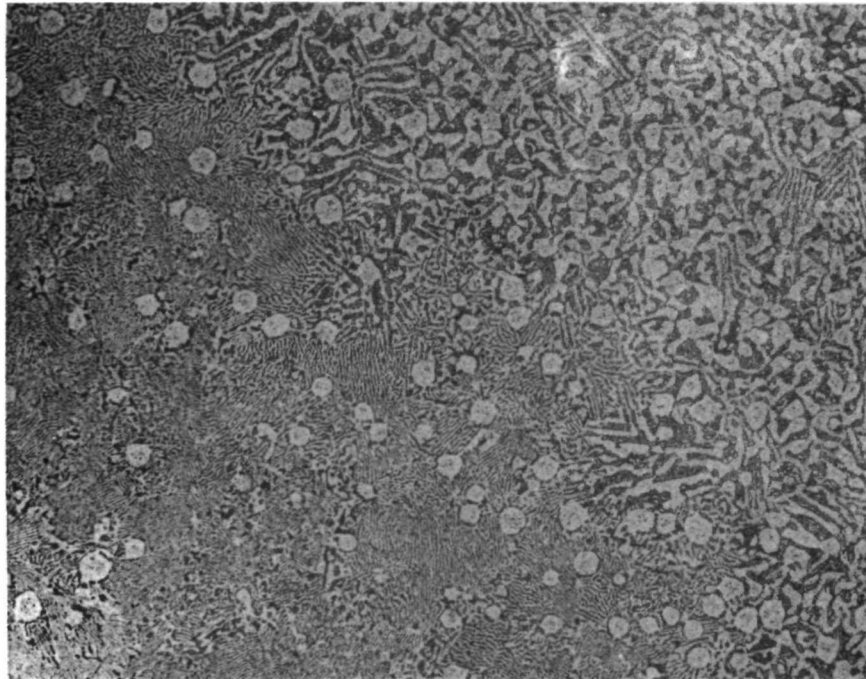


Figure 37. Duplex microstructure in transition zone at Area 3, Figure 34 (100X).

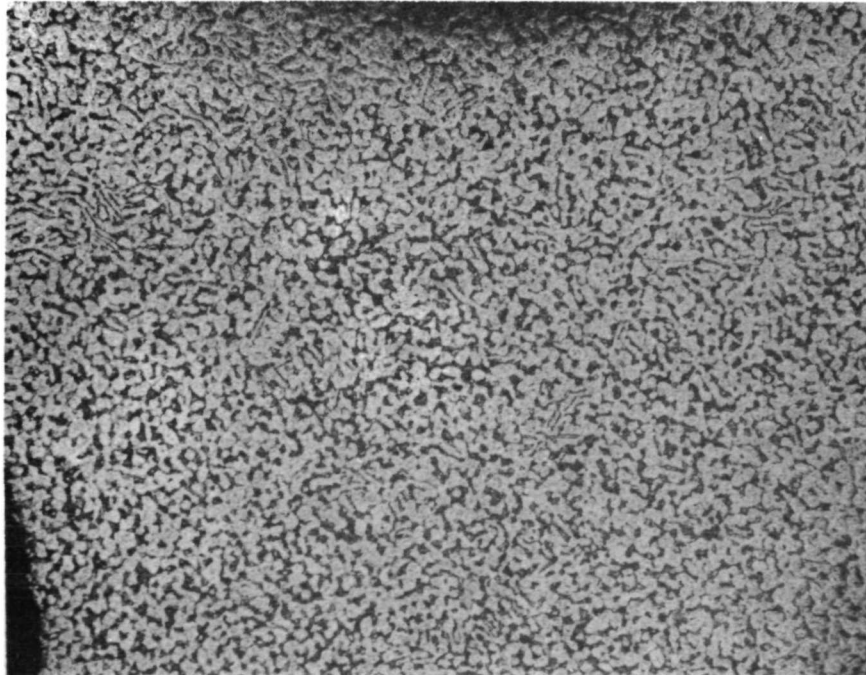


Figure 38. Unaffected microstructure at Area 4, Figure 34 (100X).



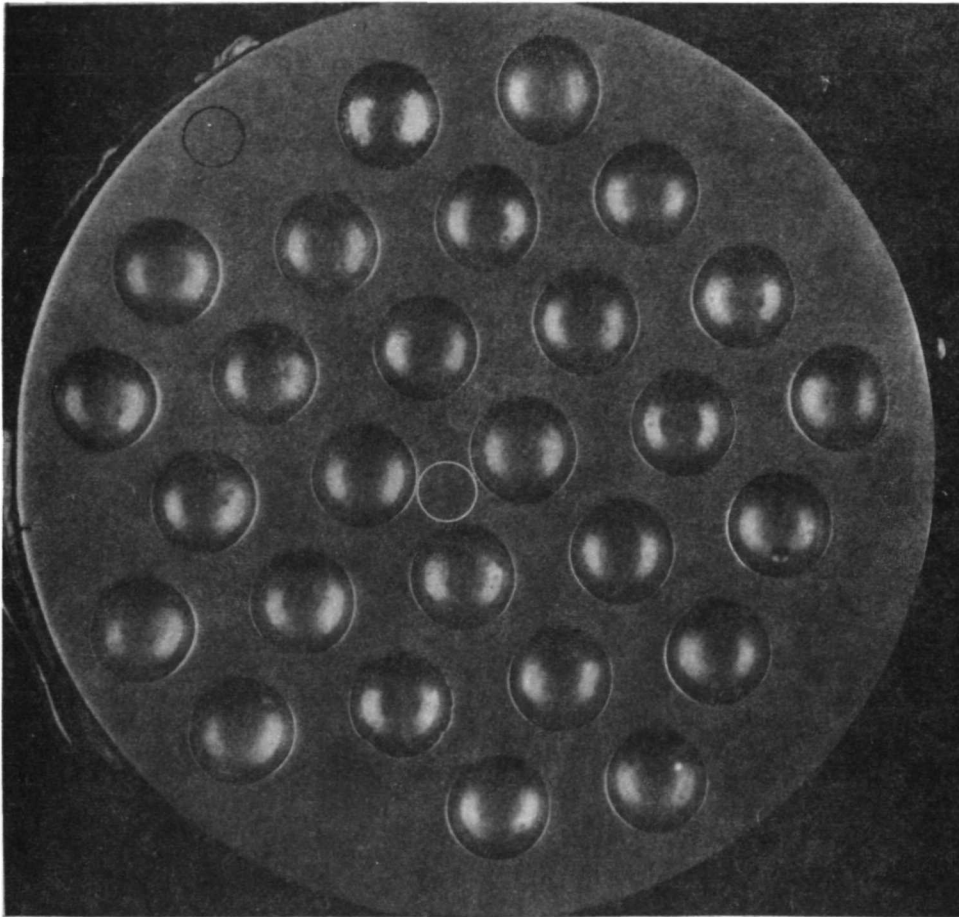


Figure 39. Surface view of as-received wafer showing macrostructure and configuration of bubbles (Enlargement of areas shown at black and white circles are shown in Figures 40 and 41, respectively) (7X).

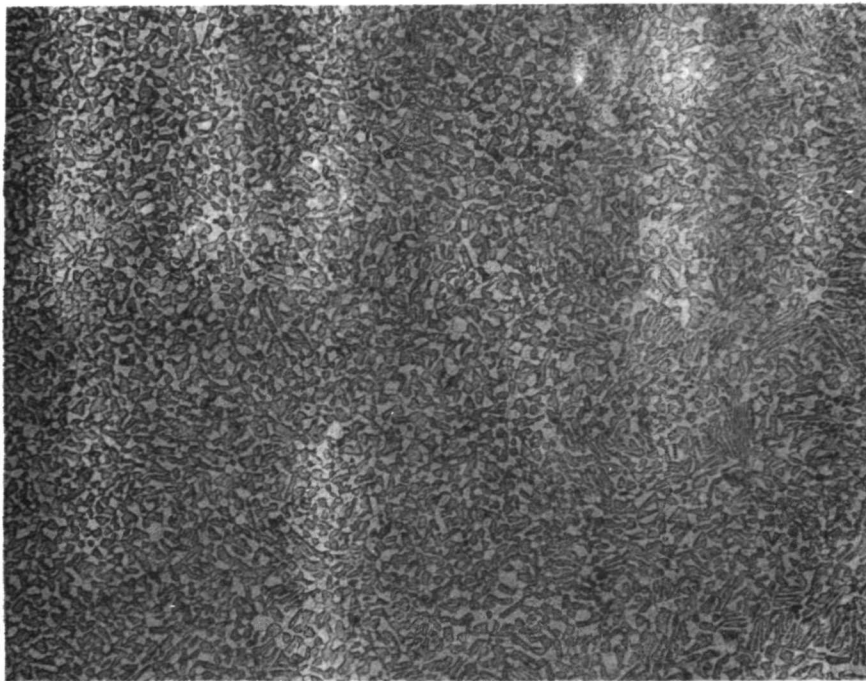


Figure 40. Surface at periphery of as-received wafer (black circle, Figure 39) (100X).

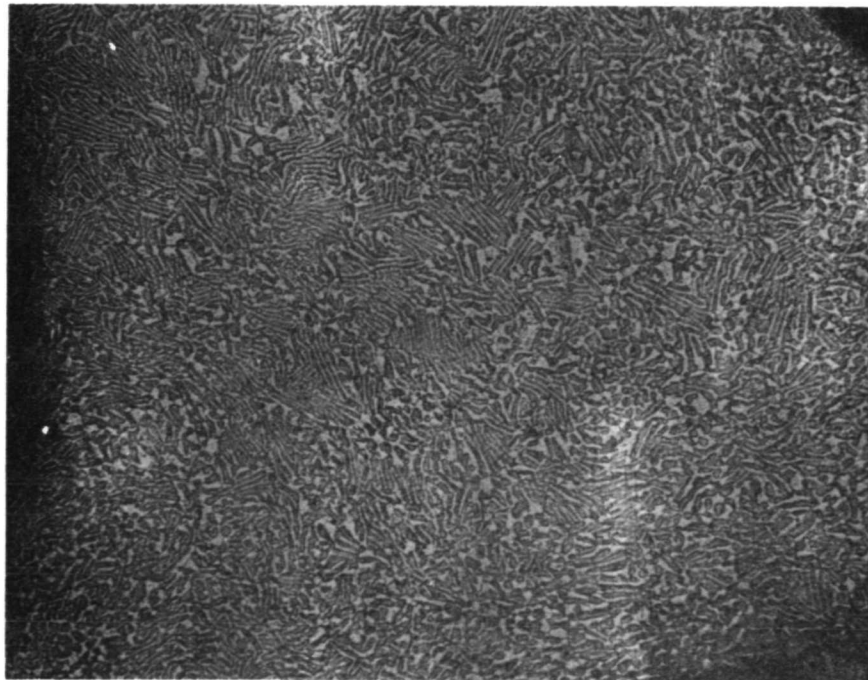


Figure 41. Surface microstructure between bubbles near center of as-received wafer (white circle, Figure 39) (100X).



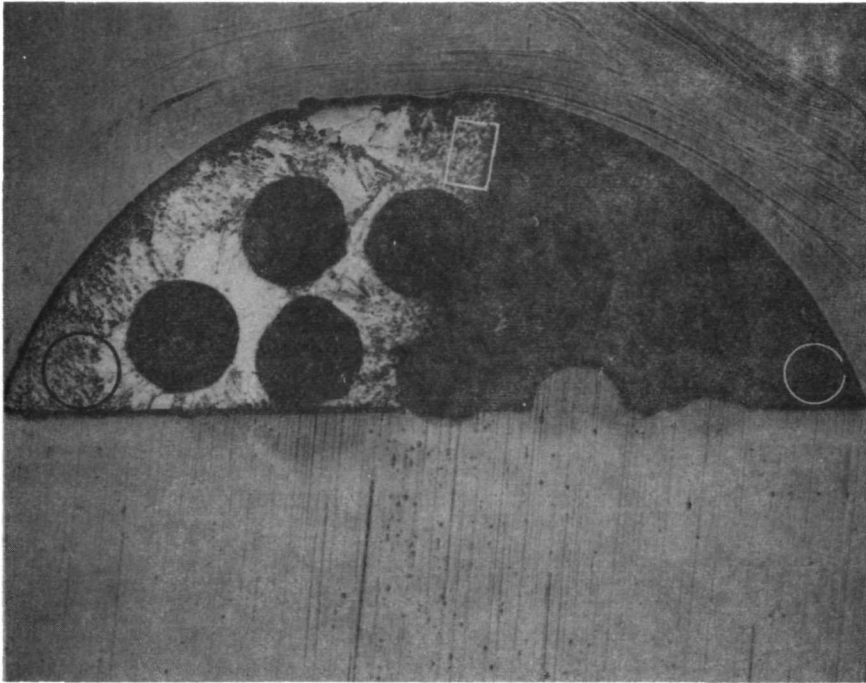


Figure 42. Transverse section exhibiting macrostructure of disk number 3 near bottom of composite (Enlargements of melted structure, transition area, and unaffected structures are shown in Figures 43 through 45) (7X).

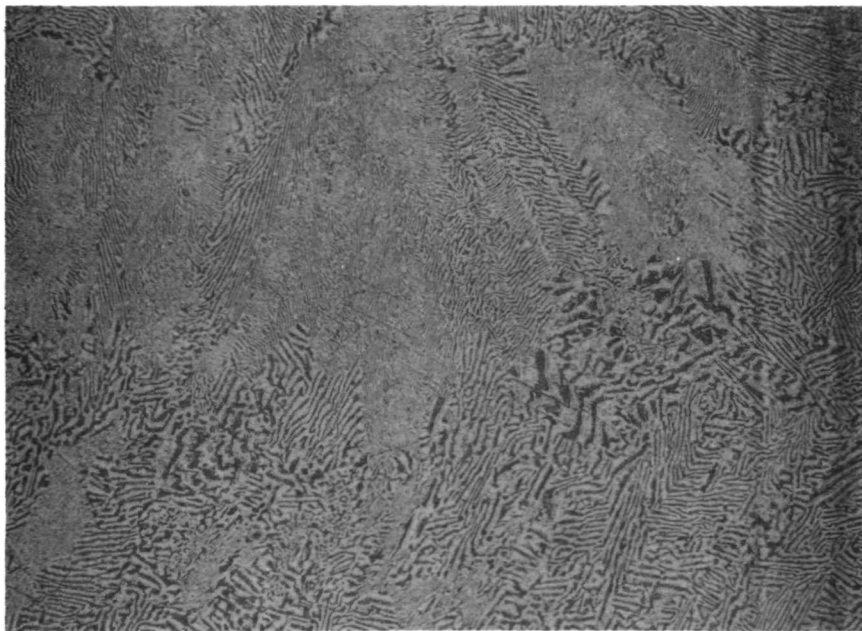


Figure 43. Enlargement of area at black circle showing recrystallized structure in melted areas (number 3 disk) (100X).

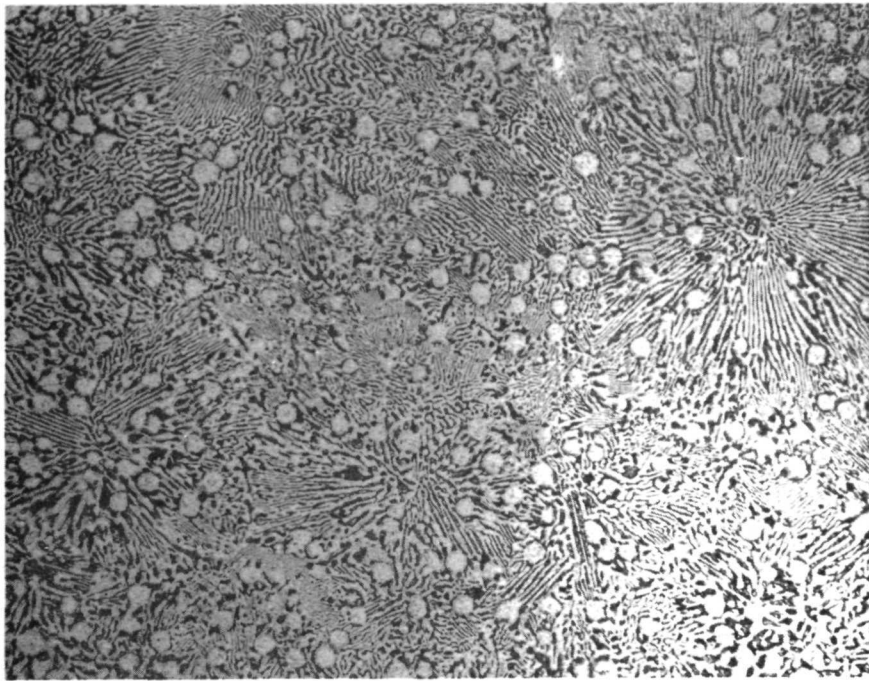


Figure 44. Enlargement of area at rectangle exhibiting microstructure of transition area between melted and unaffected structure (number 3 disk) (100X).

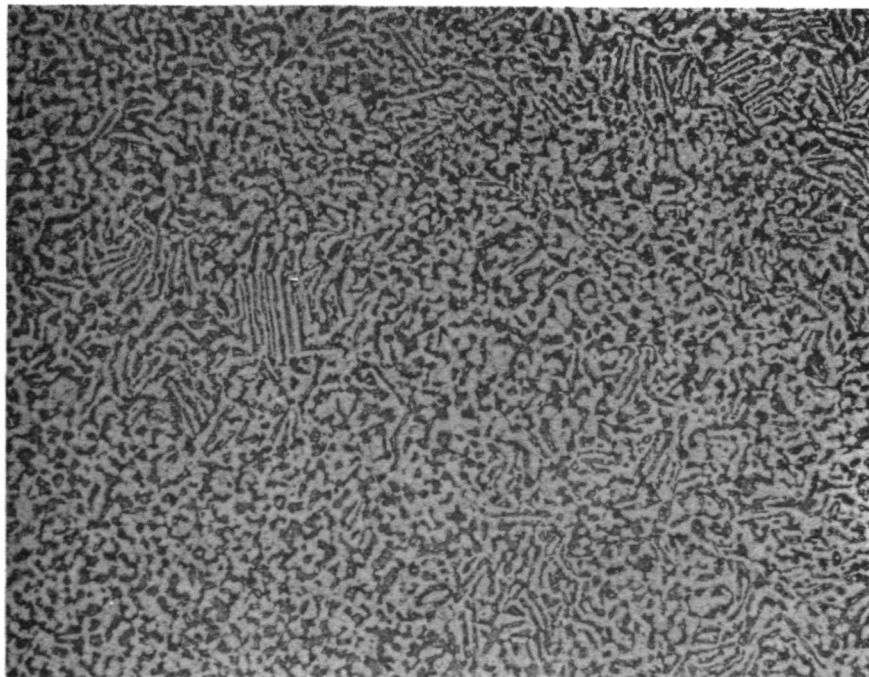


Figure 45. Enlargement of area at white circle depicting unaffected structure (number 3 disk) (100X).

## CONCLUSIONS

1. The drop tower is the preferred method of obtaining short periods of near-zero-g —  $1 \times 10^{-5}$ g.
2. Many manufacturing-in-space processes can be verified or trends of what will ultimately occur can be shown with drop tower tests.
3. KC-135 Research Aircraft flights offer little or no advantage over drop tower tests.
4. Research rockets are capable of providing periods of near-zero-g for processing materials which are 50 to 100 times longer than MSFC's 300-ft drop tower and 20 to 50 times longer than KC-135 Research Aircraft.
5. Centrifugal acceleration produced by coning (precession) after yo-yo despin of the Aerobee 170A NASA 13.113 was insignificant ( $8 \times 10^{-7}$ g) compared to that produced by the final spin rate.
6. Research rockets equipped with altitude control systems and despun to zero provide a good environment for processing materials.
7. The best location for experiments on rockets which are not despun to zero and are not equipped with altitude control is at the center of gravity of the payload/nose cone and with the centerlines of the rocket and experiment coincidental.
8. Experiments should be designed to fit standard rocket section lengths and mounting bolt circles.
9. Experiments which can be mounted on either the forward or aft side of a mounting plate have a better chance of being selected as "piggyback" experiments.
10. Experiments which are essentially self-contained and require minimum effort to integrate are most likely to be selected as "piggyback" experiments.
11. Experiments should have a minimum number of mechanical, electrical, and telemetry connections to the research rocket.

12. Experiments should be preset and should require no last minute checks and calibrations, which interfere with launch operations.

13. Experiments flown on Aerobee 170's and Black Brant VC's must meet the Aerobee 170 Vibration Specification (Appendix).

14. The results of the vibration tests must be documented and a copy will most likely be required by the center responsible for the research rocket.

15. Since there are often delays during assembly and test of a research rocket, experiments should be designed and documented so that it is not necessary for anyone to accompany the experiment to the center where it is to be integrated.

16. The integration procedure should be concise.

17. The experiment should be designed so that it can be operated by the integrating center during assembly and checkout of the rocket (e.g., the unit was shipped with a dummy capsule to the integrating center and the flight capsule was exchanged for the dummy by the experimenter during final assembly of the rocket at the launch site).

18. The ejector technique is better than the tube and reservoir technique of forming and deploying liquid metals in near-zero-g.

19. The containerless processing system began to damp the oscillations of the hollow aluminum sphere.

20. The capsule contents tended to pull away from the capsule wall as they melted, causing incomplete melting and decreasing the effectiveness of the water quench cooling system.

21. A longer holding time is needed.

22. In areas where melting occurred it was demonstrated that mixture stability in metal-gas composites processed in near-zero-g was much greater than that processed in one-g where all the gas bubbles escaped or were reduced in size because of the buoyancy forces acting on them.

## RECOMMENDATIONS

1. The capsule interiors should be plated with some material that does not repel the capsule constituents.
2. A means of increasing the cooling capability of the unit should be devised.
3. A means of reducing or eliminating the accelerations produced by spin should be devised.

# APPENDIX – AEROBEE 170 VIBRATION SPECIFICATION

## PROTOTYPE – SINUSOIDAL

Axis	Frequency	Level	Sweep Rate
Thrust Z-Z	10 - 60	3.5 g	2 octaves/min
	60 - 160	6.8 g	
	160 - 2000	11.3 g	
Lateral X-X and Y-Y	5 - 60	5.1 ips	2 octaves/min
	60 - 250	0.0 g	
	250 - 2000	11.2 g	

## PROTOTYPE – RANDOM

Axis	Frequency Range	PSD Level	Overall
Thrust Z-Z	20 - 2000	0.125	15.75 g rms
Lateral X-X and Y-Y	20 - 2000	0.228	22.5 g rms

Duration: 20 sec per axis

## FLIGHT – SINUSOIDAL

Axis	Frequency	Level	Sweep Rate
Thrust Z-Z	10 - 60	2.3 g	4 octaves/min
	60 - 160	4.5 g	
	160 - 2000	7.5 g	
Lateral X-X and Y-Y	5 - 60	5.4 ips	4 octaves/min
	60 - 250	5.3 g	
	250 - 2000	7.5 g	

## FLIGHT – RANDOM

Axis	Frequency Range	PSD Level	Overall
Thrust Z-Z	20 - 2000	0.056	10.5 g rms
Lateral X-X and Y-Y	20 - 2000	0.113	15 g rms

Duration: 10 sec per axis

APPROVAL

NASA TM X-64665

RESEARCH ROCKET TESTS RR-1 (BLACK BRANT VC)  
AND RR-2 (AEROBEE 170A): INVESTIGATIONS OF  
THE STABILITY OF BUBBLES IN PLAIN AND  
FIBER-REINFORCED METAL MELTED AND SOLIDIFIED  
IN A NEAR-ZERO-g ENVIRONMENT

By I. C. Yates and Vaughn H. Yost

The information in this report has been reviewed for security classification. Review of any information concerning Department of Defense or Atomic Energy Commission programs has been made by the MSFC Security Classification Officer. This report, in its entirety, has been determined to be unclassified.

This document has also been reviewed and approved for technical accuracy.



---

P. G. PARKS  
Chief, Metals Joining Development Branch



---

HANS F. WUENSCHER  
Assistant Director for Advanced Projects

 5/23/72

---

MATHIAS P. L. SIEBEL  
Director, Process Engineering Laboratory